Brodogradnja Volume 77 Number 4 (2026) 77412

journal homepage: www.brodogradnja.fsb.hr

Brodogradnja

An International Journal of Naval Architecture and Ocean Engineering for Research and Development

Energy costs evolution of an Adriatic cruise: Diesel, LNG and Methanol comparison

Natasha Taucer Marchesi, Enrico Del Piero, Samuele Utzeri, Donato Padolecchia, Serena Bertagna, Luca Braidotti, Vittorio Bucci*

Department of Engineering and Architecture, University of Trieste, Trieste 34127, Italy

ARTICLE INFO

Keywords:
Environmental rules
Energy costs
Methane slip
Cruise ship sustainability
Adriatic Sea

ABSTRACT

Growing environmental awareness and increasingly stringent emission limits are key drivers in modern ship design. Alongside innovations in energy conversion systems, overall ship sustainability depends on optimizing electrical systems, propulsion efficiency, and operational profiles while integrating alternative fuels. This study examines the energy costs and emission performance of a cruise ship operating in the Adriatic Sea over a 25-year horizon (2025-2050), comparing three fuel options: High Sulphur Fuel Oil, Liquefied Natural Gas, and Methanol. The analysis includes Well-to-Wake emissions, compliance costs related to the EU Emissions Trading System and FuelEU Maritime, and the evolution of the Carbon Intensity Indicator. In terms of Well-to-Wake emissions, e-Methanol achieves the lowest Green House Gasses intensity, while Natural Gas-based Methanol exceeds High Sulphur Fuel Oil due to upstream contributions. Only bio- and e-Methanol maintain Carbon Intensity Indicator compliance over the full 25-year horizon. Cost-wise, e-Methanol becomes the most competitive option by 2040, driven by avoided FuelEU penalties. The findings highlight the need for an integrated approach combining technological innovation, efficient energy management, and regulatory adaptation toward sustainable cruise operations.

1. Introduction

Maritime transport is a cornerstone of international trade, carrying over 80 % of global cargo by volume [1]. Despite its relative efficiency, the sector remains a major contributor to environmental pollution. It is responsible for around 3 % of global Green House Gasses (GHG) emissions and approximately 3-4 % of the EU's total emissions [2, 3]. These emissions include Carbon Dioxide (CO_2), Methane (CH_4), Nitrous Oxide (N_2O), Sulphur Oxides (SO_x), Nitrogen Oxides (NO_x), particulate matter (PM), and volatile organic compounds (VOCs), all of which contribute to global warming, ocean acidification, and public health risks.

In response, the International Maritime Organization (IMO) and the European Union (EU) have implemented comprehensive regulatory frameworks to mitigate the climate impact of shipping, which are

* Corresponding author.

E-mail address: enrico.delpiero@phd.units.it

https://doi.org/10.21278/brod77412

Received 02 February 2026; Received in revised form 10 June 2026; Accepted 26 June 2026
Available online 09 July 2026
ISSN 0007-215X; eISSN 1845-5859

continually evolving [4, 5]. Regulatory compliance is not merely a legal obligation but a strategic imperative. Technical standards such as Energy Efficiency Design Index (EEDI) and Energy Efficiency Existing Ship Index (EEXI) [6-9], operational metrics such as the Carbon Intensity Indicator (CII) [10-13], and economic instruments such as the EU Emission Trading System (EU ETS), the FuelEU Maritime (FuelEU) and the IMO Net-Zero Framework [4, 14-17] reflect a broader shift toward performance-based regulation. This approach encourages innovation while allowing flexibility in achieving compliance, thereby supporting a just and equitable transition for the maritime sector.

Scientific research is playing an increasingly central role in driving this transformation. Current studies focus on innovative technologies and operational strategies to reduce ship emissions. [17] provides a seminal review of approximately 150 studies on GHG reduction measures in shipping, concluding that no single technological or operational measure is sufficient to achieve meaningful reductions and that a combination of interventions is required to reach sector-wide targets.

More broadly, current studies address innovative solutions including fuel cells [18, 19], electric and hybrid propulsion systems [20], batteries [21], and supercapacitors [22], digital tools for design visualization [23, 24], Carbon Capture and Storage (CCS) technologies [25], speed reduction strategies [26, 27], energy efficiency assessment tools [28] and fuel consumption models [29, 30]. However, most of these works focus on technology-specific assessments and fleet-level scenarios, without integrating the combined financial effect of the overlapping regulatory frameworks now in force.

A first group of recent studies addresses the cost-driven selection of alternative marine fuels for cargo vessels. In [31] a cost-effective decarbonisation pathway for a deep-sea container ship is identified, assessing energy-saving technologies and alternative fuels under the EU ETS, FuelEU, CII and EEXI up to 2040, and concluding that operational measures dominate in the near term while ammonia becomes the most cost-effective fuel as the regulatory thresholds tighten. The analysis is performed through annualised projections for predefined scenarios and for a vessel whose energy demand is governed by propulsion. The study conducted in [32] extends the cost analysis to a fleet of multi-purpose heavy-lift vessels, evaluating six fuels and incorporating, in addition to the fuel cost, the penalties and credits arising from both the FuelEU Maritime Regulation and the IMO Net-Zero Framework, with compliance surpluses pooled across the fleet. The EU and IMO instruments are applied jointly, at fleet level for a cargo segment and under a static carbon price. More broadly, the inclusion of shipping in the EU ETS and the introduction of FuelEU Maritime have prompted a growing body of literature on compliance strategies and their economic impacts: in [33], the effects of the EU ETS across different ship segments and fuel pathways are assessed, finding that bio-methanol (bio-MeOH) emerges as a cost-effective compliance option for several ship types. In all these cases, however, the assessment is carried out at fleet or scenario level; none resolves the combined financial impact of the EU ETS, FuelEU Maritime and CII for an individual cruise ship along its specific itinerary and over the full compliance horizon, as the present study does.

Regarding cruise ships, studies have so far addressed emissions assessment and the economic impact of regulations but not simultaneously accounting for Well to Wake (WtW) emissions, EU ETS costs, FuelEU Maritime penalties, and CII, and when a forecast study is conducted, typically the time horizon considered is limited to a few years [34, 35]. Studies specifically addressing passenger cruise ships remain limited in scope. In [36], a WtW comparative analysis of alternative fuels is conducted, including LNG, methanol (MeOH), and ammonia, evaluating their impact on CII ratings over the period 2023-2026. While this study provides a valuable ship-level perspective on emission intensity, it does not quantify the financial impact of EU ETS allowance costs or FuelEU Maritime compliance penalties, nor does it extend the analysis beyond a four-year horizon. The study reported in [37] compares traditional fuels with seven unconventional fossil, biological and synthetic alternatives for a small luxury passenger ship, using a Matlab-Simulink model of the mechanical propulsion system and assessing technical, environmental and economic performance, including GHG emissions, CAPEX, OPEX (within which the EU ETS is accounted for), EEXI and CII. On the economic side, they adopt a broader life-cycle scope by including capital expenditure, but they do not incorporate the FuelEU Maritime penalty and their simulation targets only the propulsion plant for the fuel comparison, assuming a constant mean ship speed during the navigation from port to port. Research on cruise ships operating in the

Adriatic Sea has so far been largely confined to fleet-level emissions inventories and environmental performance assessments based on aggregate, non-ship-specific models [38, 39] without addressing long-term fuel cost competitiveness under the current EU regulatory architecture.

The literature has also examined the climate performance of the candidate fuels independently of compliance cost, an aspect that is particularly relevant for LNG whose advantage over conventional fuels is contested on account of methane slip. In [40], a comprehensive environmental and economic lifecycle assessment of Liquefied Natural Gas (LNG) as a marine fuel is conducted, demonstrating that while LNG reduces SO_x and NO_x emissions and offers cost advantages over liquid fossil fuels, its net climate benefit remains uncertain due to methane slip. Their analysis showed that fossil LNG cannot meet the IMO's 50 % GHG reduction target unless accompanied by a 35 % improvement in ship energy efficiency, and that methane slip rates must fall below 0.8-1.6 % for LNG to yield a net climate benefit over Heavy Fuel Oil (HFO). Building on this finding, the present study incorporates a sensitivity analysis on the methane slip carbon cost under the FuelEU Maritime and EU ETS frameworks, quantifying its financial impact over a 25-year horizon, an aspect not addressed in prior regulatory cost assessments.

This paper focuses on the emissions and energy costs of a 181,500 GT (Gross Tonnage) large passenger cruise ship operating in the Adriatic Sea, comparing three fuels produced from fossil and non-fossil sources. A complete fuel switch is considered here, without investigating ships equipped with multiple fuel systems. The Adriatic Sea was selected as the study region because it is a semi-enclosed sea bordered predominantly by EU member states. The objective is not to identify a single net-zero solution for the cruise sector. Rather, the study provides a policy-relevant assessment of the long-term economic and regulatory implications of fuels that are currently deployable or realistically considered in near- to mid-term transition strategies, while benchmarking them against renewable pathways. The fuels analysed are Heavy Sulphur Fuel Oil (HSFO), LNG, and MeOH. These were selected because they are currently in use or expected to be adopted in the near term. HSFO serves as the established reference fuel. LNG adoption is growing globally, including in the cruise sector. MeOH is increasingly considered as a viable option to reduce passenger ship emissions [41]. Despite being investigated within the marine decarbonisation literature [19, 42], ammonia and hydrogen were excluded for the following reasons: ammonia poses toxicity risks that make it unsuitable for passenger ships in emergency scenarios [43], while hydrogen technology for marine applications is not yet mature [44] and, due to its low volumetric energy density, would require unreasonably large space for its storage on a passenger ship or unacceptable reduction of ship range [45]. For MeOH, three production pathways are considered to capture their different impact on Well-to-Tank (WtT) emissions: natural gas-based MeOH (NG-MeOH), bio-MeOH, and e-MeOH. Marine Gas Oil (MGO) is additionally used as boiler fuel and as pilot fuel for dual-fuel engines operating on LNG and MeOH.

Emission levels, EU ETS and FuelEU Maritime compliance costs, and environmental performance indicators (GHG intensity and CII) are analysed over a 25-year horizon (2025-2050). Capital expenditures related to fuel-specific systems, such as storage arrangements, safety systems, and engine retrofits, are intentionally excluded to isolate the effect of fuel choice and regulatory mechanisms on long-term operational energy costs. The analysis is based on a simulation model specifically developed for cruise ships, requiring a complete set of inputs: environmental data, itinerary, ship geometry, power management system, passenger and crew numbers, and design electric balance [46]. Both physical and operational aspects are accounted for, and emission levels are evaluated in accordance with current regulations. Assumptions on fuel cost and carbon price evolution over the projected time frame enable a forward-looking forecast of energy costs, including regulatory penalties.

This study makes four original contributions to the literature. First, although the studies that jointly account for the EU ETS, FuelEU Maritime and CII address cargo segments, and the cruise-ship literature is so far confined to emission-intensity metrics or to short forecast horizons, this paper provides a scenario-based, long-term (2025-2050) energy cost projection for a large cruise ship that quantifies the combined financial impact of these three instruments. Second, in contrast to fleet-level or route-aggregated models, the simulation framework adopted here is ship- and itinerary-specific, incorporating environmental conditions, power management architecture, and design electric balance. Third, the study discusses the potential impact of the environmental regulatory framework on cruises in the Adriatic Sea, filling a geographic gap and identifying the dominant cost drivers shaping the energy costs through 2050. Finally, this work provides a sensitivity analysis of energy costs as a function of fuel prices and methane slip fraction.

The paper is structured as follows. Section 2 describes the current EU and IMO regulatory framework and provides an overview of the propulsion and fuel storage technologies considered. Section 3 presents the methodology, including the simulation algorithm for fuel consumption, the environmental assumptions, the formulation for emission and energy cost assessment and the sensitivity analysis. Section 4 describes the test ship, itinerary, and environmental conditions. Section 5 presents and discusses the results in terms of emission levels, penalty amounts, energy costs, and CII evolution. Section 6 summarises the main conclusions and outlines directions for future work.

2. General background

In the following, only the regulatory elements and the technical aspects strictly required to frame the subsequent analysis are presented. Accordingly, the section does not aim to provide a comprehensive review of current regulations and technologies but is limited to the elements necessary to support the methodological framework and the discussion of results.

2.1 International Regulations

The decarbonization of international shipping is governed by a multi-layered regulatory architecture, primarily led by the IMO and increasingly complemented by regional frameworks such as those of the EU. These regulations aim to reduce GHG emissions through a combination of technical standards, operational metrics, and market-based mechanisms, while also preparing the sector for a transition to zero and near-zero-emission fuels.

Along regulatory history exists with respect to NO_x, primarily through the IMO, which has progressively tightened emission limits under Annex VI of the MARPOL Convention since the early 2000s. These tiered standards (Tier I–III) have played an important role in limiting air pollutants, particularly in Emission Control Areas (ECAs). According to MEPC.391(81) [47], the GHGs addressed within the IMO framework include CO_2, CH_4, and N_2O. Methane and methane slip are therefore explicitly considered in the calculation of the GHG index. In the maritime sector, methane emissions primarily originate from methane slip in dual-fuel engines operating on LNG, as well as from incomplete combustion processes associated with other fuel types. The EU also considers CO_2, CH_4, and N_2O as GHGs and includes them in the FuelEU and EU ETS calculations [4, 14].

However, there are differences between the EU and IMO approaches. In this regard, it is essential to distinguish between WtT emissions, which occur during the extraction/production, processing, and delivery of marine fuels, and Tank-to-Wake (TtW) emissions, which are released during onboard combustion. Together, these dimensions form the WtW approach, providing a more holistic understanding of the climate impacts of different fuel pathways and operational profiles. Both the EU and the IMO calculate GHG intensity considering WtW emissions; however, the former foresees a penalty system linked to the GHG index while the IMO does not. This divergence in classification and regulatory focus between the IMO and the EU has significant implications for the alignment of international and regional decarbonization strategies. Moreover, the IMO framework does not always consider the WtW emissions in its index calculations: for the assessment of CII and EEDI, IMO only accounts for the TtW CO_2 emissions, ignoring CH_4, N_2O, and WtT contributions, adding another layer of regulatory divergence. In the following, the current rules are briefly analysed to provide a solid framework for the current study.

2.1.1 IMO Regulations

The IMO has developed a phased regulatory framework to reduce GHG emissions from international shipping. The Initial GHG Strategy set targets of at least 40 % reduction in CO_2 emissions per transport work by 2030 and at least 50 % in total GHG emissions by 2050, both relative to 2008 levels [5]. Short-term measures (2018-2023) focus on technical instruments: the EEDI, mandatory for new buildings since 2013 [6, 7]; the EEXI, applicable to existing ships since 2023 [8, 9]; and CII. All these technical instruments establish minimum energy efficiency thresholds by ship type and size. The medium-term phase (2023–2030) introduces a set of measures comprising a technical component (a GHG Fuel Standard to regulate fuel GHG intensity) and an economic component (market-based mechanisms such as carbon pricing or a GHG levy), designed to internalise emission externalities while ensuring fairness for developing states [48]. The 2023 revised Strategy further strengthened these ambitions with indicative checkpoints of 20-30 % total GHG reduction by 2030 and 70-80 % by 2040 (relative to 2008), targeting net-zero emissions by or around 2050 adopting a WtW accounting approach, covering the full lifecycle of marine fuels from production to combustion, to prevent carbon leakage and avoid displacement of emissions to other sectors [5]. More recently, at its 83rd session [17], the IMO approved the Net-Zero Framework, a proposed new Chapter 5 of MARPOL Annex VI that introduces a mandatory GHG Fuel Intensity (GFI) standard, on a well-to-wake basis, for ships of 5,000 GT and above from 2028. The attained GFI is to be reduced along two trajectories: a Base target and a more ambitious Direct Compliance target relative to a 2008 reference value of 93.3 gCO_2eq/MJ. Non-compliance is settled through remedial units, over-compliant ships earn surplus units, and the resulting revenues are directed to an IMO Net-Zero Fund. Formal adoption was subsequently deferred, with negotiations expected to resume in 2026.

2.1.1.1 Carbon Intensity Indicator

The CII, introduced under MARPOL Annex VI and formalised through resolutions MEPC.346(78) and MEPC.355(78) [12, 13], is mandatory since January 2023 for ships above 5,000 GT on international voyages, quantifying operational carbon efficiency as grams of CO_2 per capacity-mile. Ships receive an annual rating from A to E with progressively stricter thresholds; a minimum C-rating is required for compliance [12]. An E-rating in any single year, or a D-rating for three consecutive years, triggers the obligation to develop a Corrective Action Plan under the Ship Energy Efficiency Management Plan (SEEMP) Part III, subject to third-party audit [49]. CII assessments are based on fuel consumption data submitted through the IMO’s Data Collection System (DCS) and require operators to account for a range of technical and operational parameters, including fuel type, distance travelled, and vessel capacity as [10]:

$$CII = \frac{Annual\ emissions}{Transport\ work} \tag{1}$$

where annual emissions account only for the TtW CO_2 ones (so not taking account of CH_4, N_2O and possible slip) and the transport work is given by the product of the actual sailed distance in nautical miles and the measure of the size of the vessel (Deadweight tonnage, DWT, or GT, according to the ship type). This value, called attained CII (CII_A) is then benchmarked against a ship-type-specific Required CII (CII_R) and adjusted by annual reduction factors (5 % in 2023, increasing by 2 % per year to at least 11 % by 2026) [50]. A significant methodological limitation is that the CII accounts solely for CO_2 mass, excluding CH_4, N_2O, and methane slip, which might lead to a systematic underestimation of climate impact, particularly for LNG-fuelled ships [51, 52]. Further criticisms concern the use of nominal rather than actual cargo capacity as the denominator, which raises fairness and comparability concerns for ships on irregular or specialised routes, and the framework's limited sensitivity to real-world variability such as weather conditions and trading patterns [53-55]. In particular, voyage correction factors and exemptions (codified under MEPC.355(78)) are still under refinement, and some scholars argue that the CII may inadvertently disadvantage certain ship types [56]. The planned 2025 review is expected to address some of these gaps and may introduce stricter enforcement mechanisms or financial penalties for non-compliance.

2.1.1.2 Greenhouse Gas

The IMO's GHG strategy, not yet in force, targets the accelerated adoption of zero or near-zero GHG emission technologies and alternative fuels, which are expected to represent at least 5 %, ideally 10 %, of the sector's total energy consumption by 2030 [5]. Central to this approach is the WtW emissions calculation, which integrates both WtT and TtW components. This dual-part structure is formalised as [47]:

$$GHG_{WtW} = GHG_{WtT} + GHG_{TtW} \quad (2)$$

where emissions are expressed in grams of CO_2 equivalent per megajoule of Lower Calorific Value (LCV) of the fuel or electricity used onboard [57]. The framework includes provisions for emissions avoided through onboard carbon capture (OCCS) and underpins the Fuel Life Cycle Label (FLL) certification system, enabling consistent comparison across fuel types and production pathways. Operationally, it requires shipowners, operators, and fuel suppliers to integrate lifecycle GHG profiles into decision-making and to ensure data traceability and third-party verification, thereby promoting low-carbon alternatives such as e-MeOH, green ammonia, and sustainable biofuels. From a policy perspective, the codification of GHG intensity formulas provides a robust basis for market-based measures such as carbon pricing, while the modular design of the system allows future adaptation to scientific and technological advances, ensuring long-term coherence with the Paris Agreement and the UN 2030 Agenda [58].

2.1.2 EU Regulations

The EU has embedded maritime transport into its broader decarbonization framework, going beyond IMO requirements. Anchored in the European Green Deal and the "Fit for 55" package (2021), the EU targets at least 55 % net GHG reduction by 2030 relative to 1990 levels, with the overarching goal of climate neutrality by 2050 [59]. Maritime shipping, historically regulated primarily through the IMO [2], has been brought into regional climate policy on three grounds: its heavy reliance on fossil fuels (predominantly Heavy Fuel Oil, HFO, and MGO) [60], the projected growth of emissions driven by increasing global trade volumes [61], and the sector's untapped potential for efficiency improvements and fuel substitution [62]. The EU's unilateral action also reflects the perception that IMO progress is insufficient to meet the Paris Agreement's 1.5 °C target, and a strategic objective to stimulate technological innovation and exert normative influence on global regulatory developments. Two cornerstone instruments have been introduced: the extension of the EU ETS to maritime transport, as a market-based emission pricing mechanism, and the FuelEU Maritime regulation, which sets binding GHG intensity limits for onboard energy use. Together, they constitute a dual economic and technical approach aligned with the Union's long-term climate neutrality objective. Notably, EU regulations have in many respects anticipated the IMO strategy; consequently, the analysis of EU-regulated routes already offers a forward-looking indication of the regulatory and economic dynamics that may unfold at a global scale once IMO measures are fully implemented.

2.1.2.1 EU ETS

The EU ETS was extended to maritime transport through Regulation (EU) 2023/957, amending Directive 2003/87/EC, with effect from January 2024 [14]. Allowance surrender obligations are being phased in gradually: 40 % of verified emissions in 2024, 70 % in 2025, and 100 % from 2026, providing the sector with time to adapt operations and explore alternative fuels [63]. The regulation applies to ships of 5,000 GT and above on commercial voyages, covering 100 % of emissions from intra-EU routes (including Norway and Iceland) and 50 % of emissions from voyages entering or leaving EU ports. This is a geographic scope designed to encompass EU-connected international activities while avoiding excessive extraterritorial application. Currently limited to TtW CO_2 emissions, the framework will progressively broaden its coverage: monitoring and reporting of CH_4 and N_2O became mandatory from January 2024, with the corresponding allowance surrender obligations for these gases entering into force from 2026, enabling a more comprehensive assessment of shipping's climate impact.

2.1.2.2 Fuel EU

The FuelEU Maritime regulation, adopted as part of the "Fit for 55" package and entering into force in 2025 [4], constitutes the technological and operational counterpart to the EU ETS: whereas the latter prices carbon emissions, FuelEU Maritime sets binding performance standards for the GHG intensity of onboard energy, driving structural transformation in fuel choices and propulsion systems. The compliance metric is based on WtW GHG intensity, expressed in gCO_2eq/MJ, encompassing both upstream (WtT) and combustion

(TtW) contributions, and includes a remuneration factor for wind-assisted propulsion. The regulation introduces a stepwise reduction trajectory relative to the 2020 baseline: 2 % by 2025, 6 % by 2030, 14.5 % by 2035, 31 % by 2040, 62 % by 2045, and 80 % by 2050. Unlike measures that only account for direct TtW emissions, FuelEU Maritime is based on the WtW GHG intensity of energy carriers, thereby encompassing both upstream emissions (extraction, production, and transport) and downstream combustion. The compliance metric, i.e., GHG intensity, is expressed as [4]:

$$GHG_{actual} = f_{wind}(WtT + TtW) \tag{3}$$

where WtT is Well to Tank contribution, TtW is Tank to Wake contribution, and f_{wind} is the remuneration factor for wind-assisted propulsion defined as [4]: equal to 0.99 if $P_{wind}/P_{prop} = 0{,}05$; 0.97 if $P_{wind}/P_{prop} = 0{,}1$; 0.95 if $P_{wind}/P_{prop} \geq 0{,}15$. This framework applies across a wide range of energy carriers, from conventional HFO to alternatives such as bio-MeOH, hydrogen, ammonia, and synthetic e-fuels. Moreover, for Renewable Fuels of Non-Biological Origin (RFNBOs), i.e., all fuels other than biofuels and biogas which are produced from renewable sources other than biomass, the regulations provide that only the 50% of WtW emission considered until 2033 with the aim of encouraging their adoption [4, 64]. Compliance is assessed at the company fleet level on an annual basis; failure to meet the applicable GHG intensity limit results in financial penalties proportional to both the degree of non-compliance and total energy consumed. The regulation further mandates the use of Onshore Power Supply (OPS) for container and passenger ships at major EU ports by 2030, addressing both climate and air quality objectives. Although the FuelEU Maritime Regulation and the IMO GFI standard are structurally similar, they differ in scope, reference basis and flexibility: the GFI applies globally against a 2008 baseline of 93.3 gCO_2eq/MJ, whereas FuelEU applies within the EU/EEA against a 2020 baseline of 91.16 gCO_2eq/MJ and, unlike the IMO mechanism as approved, allows compliance surpluses to be pooled across vessels

2.2 Technology

Marine propulsion has historically relied on internal combustion engines fuelled by fossil fuels, predominantly in two-stroke slow-speed or four-stroke medium/high-speed diesel configurations [65]. The tightening of international regulations, notably MARPOL Annex VI, has accelerated the transition toward cleaner and more efficient systems [66]. Contemporary innovations follow three interrelated directions: efficiency, emissions reduction, and operational flexibility. Efficiency gains derive from advanced electronic control systems [67-69], waste-heat recovery [70], and hybrid propulsion architectures [71]. Emissions reduction is pursued through alternative fuels (LNG, biofuels, and synthetic options) and after-treatment technologies such as Selective Catalytic Reduction (SCR) [72, 73], Diesel Particulate Filters (DPF) [74], and scrubbers [75]. Operational flexibility is enhanced by dual-fuel engines and application-specific propulsion designs [26, 76], while advances in lightweight high-performance materials further reduce fuel consumption [76]. These directions are not independent: innovations in control systems, fuels, hybridisation, and materials reinforce one another, defining a coherent technological trajectory aligned with decarbonization goals. Fuel choice also directly affects onboard storage arrangements: while HFO and MGO can be stored in conventional structural tanks, LNG requires cryogenic prismatic or cylindrical tanks (IMO Type I, II, or III), and MeOH requires inert-gas-filled cofferdams, both resulting in reduced tank capacity and ship range, with particularly significant implications for cruise ships [45]. An emerging solution for MeOH is the Methanol Superstorage technology, which replaces cofferdams with a Sandwich Plate System (SPS) consisting of a metal-elastomer-metal composite with A60 fire rating, minimising capacity penalties; however, this technology remains approved in principle by Classification Societies and is not yet widely commercialised [77, 78]. The main fuels considered in this study (HSFO, MGO, LNG, and MeOH) are introduced in the following paragraphs, with their principal characteristics summarised in Table 1.

Table 1 Main characteristics of the fuels tested [5, 79]

Fuel	Density [t/m³]	Volumetric Energy Density [GJ/m³]	Gravimetric Energy Density [GJ/t]	LCV [MJ/kg]	Flash Point [°C]	Tmax bunker [°C]	Type of bunker
HSFO	0.980	40.0	40.816	40.5	>60	60	Structural Tank
MGO	0.890	36.6	41.12	42.7	>60	40	Structural Tank
LNG	0.460	23.4	50.86	49.1	<-180	-162	Cryogenic tank Type I, II, III*
MeOH	0.748	15.8	21.12	19.9	11-12	20	Structural Tank with cofferdams

*Cryogenic tank Types I, II, and III refer to the IMO IGF Code classification for independent LNG tanks with different structural configurations and pressure capabilities.

2.2.1 Diesel

Marine diesel fuels are classified into three principal categories: MGO, Marine Diesel Oil (MDO), and HFO, each with distinct thermophysical and environmental characteristics. HFO is further subdivided by sulphur content [80]: HSFO, the most widely used type, and the one considered in the present study, requires the installation of exhaust gas scrubbers [5]; Very Low-Sulphur Fuel Oil (VLSFO) is employed outside Sulphur Emission Control Areas (SECAs) to avoid scrubber use; and Ultra Low-Sulphur Fuel Oil (ULSFO) is increasingly adopted in response to the growing number of SECAs worldwide [81]. Key parameters governing the design and operation of onboard fuel storage, injection, and treatment systems include density, flash point, combustion behaviour, LCV, and WtT and TtW emission coefficients.

2.2.2 LNG

LNG has emerged as a major alternative marine fuel due to its compliance with stringent environmental regulations and its favourable thermophysical properties. Produced via cryogenic liquefaction at approximately −162 °C [82], LNG consists primarily of methane and offers high specific energy on a mass basis, along with well-defined flammability limits and a high autoignition temperature that make it suitable for marine use. Its lower volumetric energy density, however, requires larger onboard storage tanks compared to conventional diesel fuels. In combustion, LNG exhibits high thermal efficiency and clean-burning behaviour and is compatible with dual-fuel slow-speed diesel engines, lean-burn Otto-cycle units, and gas turbines [83]. Onboard integration requires cryogenic insulated tanks, vaporizers, double-walled piping, and dedicated pressure and temperature management systems [84], as well as mandatory gas detection, ventilation, and explosion protection arrangements under the IGF Code [85]. A key operational challenge is methane slip (the release of unburned methane under certain operating conditions in dual-fuel engines), which requires mitigation through advanced engine tuning [86]. From an operational perspective, LNG reduces maintenance costs due to the absence of soot and its cleaner combustion profile [87] and can be cost-competitive where bunkering infrastructure is well-developed [88]. Adoption is nonetheless constrained by higher capital investment, specialised safety requirements, crew training obligations, and uneven bunkering availability across ports, with truck-to-ship, shore-to-ship, and ship-to-ship transfer methods each presenting distinct technical and regulatory considerations [89].

2.2.3 Methanol

MeOH has attracted growing interest as a marine fuel due to its regulatory compliance and decarbonization potential. Unlike LNG, MeOH is liquid at ambient conditions and contains intrinsic oxygen in its molecular structure, which shapes its combustion behaviour; these properties allow storage and handling through conventional liquid-fuel infrastructure without cryogenic systems, simplifying bunkering and onboard fuel management. MeOH can be produced from multiple feedstocks: conventional fossil-based MeOH is synthesised from natural gas or coal via steam reforming or gasification [90]; bio-MeOH is derived from renewable biomass resources through gasification or reforming, offering significant lifecycle GHG reductions [91]; and e-MeOH is produced from captured CO_2 and renewable hydrogen via water electrolysis powered by green electricity, representing a promising carbon-neutral pathway aligned with global decarbonization targets [92]. Renewable production routes, including biomass gasification, waste-to-methanol and power-to-methanol, are advancing rapidly [93]. MeOH is less energy-dense than conventional marine distillates, requiring larger tanks or more frequent refuelling. Its low flash point classifies it as a low-flashpoint fuel under the IGF Code [85], mandating enhanced safety measures such as double-wall piping, leak detection, inertisation, and explosion-proof ventilation; however, its relatively high autoignition temperature and wide flammability range enable stable combustion in internal combustion engines. In combustion, MeOH produces no SO_x, virtually eliminates particulate matter, and generates lower NOx emissions than HFO [94]; crucially, it avoids methane slip, a notable advantage over LNG. Operationally, MeOH reduces engine maintenance due to the absence of soot and sulphur-related corrosion and can be integrated into existing liquid-fuel port infrastructure with appropriate adaptations [95], though its toxicity necessitates stringent handling protocols and specialised crew training [94]. Economically, MeOH remains costlier than HSFO but is competitive with MDO and MGO where supportive policies or established supply chains are in place [96].

3. Methodology

In this section, the applied methodology is presented. First, the itinerary modelling and the simulation model are described, together with related assumptions and simplifications. Then, the fuel characterisation and the emissions assessment are described, following the indications of international regulations, specifically the EU and IMO rules. Finally, the energy costs calculation methodology is presented, along with the assumptions and simplifications needed to forecast costs out to 2050.

3.1 Itinerary Modelling

The cruise ship's itinerary is modelled through legs connecting the subsequent ports of call, defining the overall route. More specifically, each leg is divided into sublegs: i.e., straight segments characterised by constant speed, direction, loading condition, and environmental conditions. Each subleg falls under one of the following four phases, defining the ship's operational status:

1. **Navigation**: The vessel operates at or near cruising speed in open sea or shallow waters. This constitutes the primary operational phase. During this phase, a minimum of two diesel generators must remain online to ensure the continuous availability of propulsion and steering systems.
2. **Transit**: This phase occurs as the vessel approaches or departs from port. The vessel maintains a reduced speed to facilitate pilot boarding and to ensure safe passage through canals, restricted waters, or shallow approaches to the berth. An additional generator, beyond the number required in the Navigation phase, is typically brought online to guarantee safe execution of emergency manoeuvres if necessary.
3. **Manoeuvring**: The vessel conducts low-speed manoeuvres to approach the berth and complete mooring operations. Bow and stern thrusters are commonly employed in this phase. The generator configuration is generally equivalent to that of the Transit phase, ensuring adequate power availability for thruster operation and control systems.
4. **Port Stay**: While the vessel is moored alongside the berth, propulsion systems are inactive. However, hotel load demands must still be met, either through onboard diesel generators or via OPS, where available. In this phase, operation with a single generator is permitted and typically sufficient to sustain the hotel load, as a portion of passengers and crew disembark.

For annual estimations, it is assumed that the itinerary is repeated identically throughout the year, excluding a two-week maintenance period. Accordingly, yearly figures for fuel consumption, emissions, and related parameters are obtained by multiplying the values from a single voyage by the number of annual repetitions.

3.2 Simulation Algorithm

The model used for the computations is a deterministic, model-based estimation framework specialised for cruise ships and aims to estimate fuel consumption and emissions given a limited number of input data [46]. In this context, the term "simulation" denotes a time-resolved physics-based modelling approach rather than numerical simulation. Such inputs include the itinerary, the ship's geometric characteristics, environmental data, the power management system, the number of passengers and crew, and the design electric balance. The modelling involves both the physical and operational aspects, i.e., the actual heading and resistance evaluation, the loading condition, and the power system. Moreover, the emissions are assessed according to the currently applicable regulations.

For the purposes of this study, the algorithm (originally designed to support probabilistic analyses via multiple Monte Carlo simulations) is employed in a deterministic manner. A single simulation is conducted under average environmental conditions, specifically by considering mean values for wind and wave-induced resistance. The underlying assumptions are detailed below. The algorithm is developed in a MATLAB environment and more details on the simulation stages are reported in [46], together with validation against real operational data.

3.2.1 System of equations

For clarity, the following equations summarise the hydrodynamic and power-balance model used to estimate propulsion demand and fuel consumption; only the core relations needed to reproduce the modelling steps are reported here.

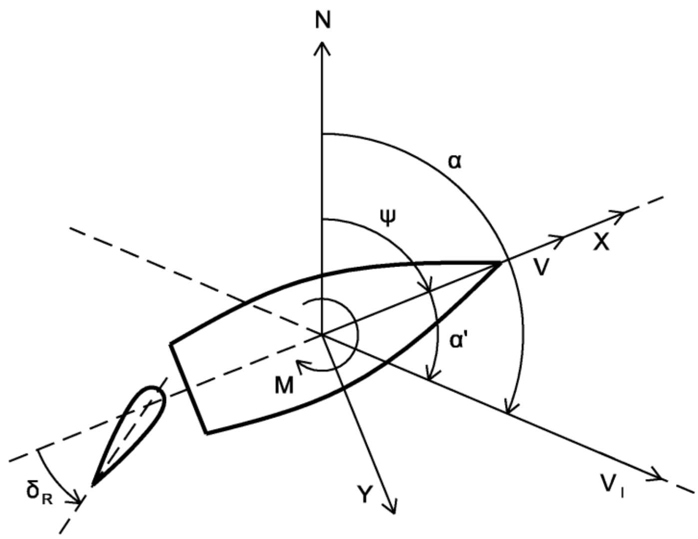

Fig. 1 Ship-fixed reference system [46]

To determine the ship's equilibrium during a specific subleg of its route, all acting forces are considered within a reference frame fixed to the ship (Figure 1). Given the speed over the ground and the course (known from the itinerary), the unknowns to solve for are the ship's heading (ψ), the rudder angle (δ_R), and the effective longitudinal force exerted by the propeller (R_T), which balances all longitudinal components of other forces. A 3-degree-of-freedom (3-DoF) model defines equilibrium through three nonlinear equations accounting for longitudinal forces (*X*), lateral forces (*Y*), and yaw moment (*M*), which originate from hydrodynamic effects (*hydro*), including interaction with the current [97], wind resistance (*wind*) [98], added resistance (*wave*) [99], and rudder forces (*rud*) [100], all depending on the ship's heading and rudder angle. The equilibrium equations are as follows:

$$\begin{cases} 0 = R_T + X_{hydro}(\psi) + \overline{X}_{wave}(V_S) + \overline{X}_{wind} + X_{rud}(\psi, R_T, \delta_R) \\ 0 = Y_{hydro}(\psi) + Y_{rud}(\psi, R_T, \delta_R) \\ 0 = M_{hydro}(\psi) + M_{rud}(\psi, R_T, \delta_R) \end{cases} \tag{4}$$

Here, $\overline{X}_{wave}$ and $\overline{X}_{wind}$ are the average longitudinal forces due to waves and wind, as determined in Section 3.2.2. Additional details about hydrodynamic effects and rudder forces are fully detailed in [46]. The system is solved using a trust-region dogleg algorithm based on the interior-reflective Newton method and preconditioned conjugate gradients [101-104]. The solution tolerances are set to 0.001 N for forces and 0.001 Nm for moments. The initial condition assumes the ship's heading equals its true course and that the rudder angle is zero.

3.2.2 Average Environmental Conditions

Since the Adriatic Sea is characterised by not excessive variations in currents and weather conditions, it was chosen to adopt simplified and annual mean values to characterise the environmental conditions in which the ship operates. These mean values are then used to calculate the mean value of current, added wave, and wind resistance, which are used to assess propulsion demand for each subleg of the itinerary.

For the sea current, an annual average value of the velocity was calculated based on the Pilot Charts [105] that provide the monthly average speed and direction of ocean currents for every sea worldwide.

The sea state and wind statistics are derived from [106], which provides wave and wind atlases for the Adriatic Sea. The data used to construct the atlases were extracted from the World Waves Database, covering the period from September 1992 to January 2016. The atlases report the joint frequency of occurrence of waves characterised by a specific pair of significant wave height H_s and zero-crossing period T_z. Also, atlases give the joint frequency of occurrence of wind by pairs of significant wave height H_s, and wind speed u_w. These are provided both for individual regions (Northern, Central, and Southern Adriatic) and for the entire Adriatic Sea.

The wind-induced forces are computed using the relative wind velocity, following the method proposed by [98]. The resulting resistance is then averaged according to the wind occurrence frequency as follows:

$$\overline{X}_{wind} = \frac{\sum_j X_{wind,j}\, f(u_w, H_s)_j}{\sum_j f(u_w, H_s)_j} \tag{5}$$

Here, $f(u_w, H_s)_j$ is the frequency of occurrence of the j-th wind state given the pair composed of wind velocity u_w and significant wave height H_s whereas $X_{wind,j}$ is the related wind resistance calculated considering the relative speed. Finally, the added wave resistance transfer function $RAW/\zeta^2(\omega_e, \psi)$ is calculated, where ω_e is the encounter frequency [99]. The computed resistance depends on the encounter angle χ, sea state, hull geometric characteristics, and ship speed V_S. The sea state is modelled by means of the Pierson-Moskowitz spectrum $S_\zeta(\omega_e, H_s, T_z)$, which utilise two parameters: the significant wave height, H_s, and the zero-crossing period, T_z [107]. The wave force is then evaluated as [108, 109]:

$$X_{wave}(V_S, \chi, H_s, T_z) = -2\int_0^\infty \frac{R_{AW}}{\zeta^2}\big(\omega_e(V_S, \chi)\big) S_\zeta(\omega_e(V_S, \chi), H_s, T_z)\, d\omega_e \tag{6}$$

For each sea state, the added wave resistance $X_{wave}(V_S, \chi, H_s, T_z)$ is calculated for every combination of speed, encounter angle and sea state. This resistance is then averaged over all encounter angles for each i-th ship speed and j-th sea state:

$$\overline{X}_{wave_{ij}} = \frac{1}{N}\sum_{k=1}^{N} X_{wave}\left(V_{S_i}, \chi_k, H_{s_j}, T_{z_j}\right) \tag{7}$$

Here, χ_k is the k-th encounter angle, and N the total number of encounter angles considered. The encounter angles considered space from 0 to 360 degrees, with increments of 10 degrees. Subsequently, for each speed, a weighted average of the resistance is computed based on the frequency of occurrence of each sea state as:

$$\overline{X}_{wave_i} = \frac{\sum_j \overline{X}_{wave_{ij}} f\left(H_{s_j}, T_{z_j}\right)}{\sum_j f\left(H_{s_j}, T_{z_j}\right)} \tag{8}$$

Here, $f\left(H_{s_j}, T_{z_j}\right)$ is the frequency of occurrence of the j-th sea state. In this way, the mean added wave resistance is obtained for each ship speed.

3.2.3 Resistance correction

In addition to resistance due to environmental conditions, the model includes corrections to the ship's resistance curve to account for variations in the loading condition, hull fouling, the use of stabilising fins, and navigation in shallow water.

At each sub-leg, the ship's loading condition is updated based on the filling levels of fuel, fresh water, and grey/black water tanks. This results in changes in displacement and therefore in the ship's draft, which alters the wetted surface area and resistance. The corresponding correction to the resistance curve is applied using the Admiralty formula [46].

Hull fouling is a significant factor in the assessment of hydrodynamic resistance, as its progressive accumulation increases surface roughness and effective wetted area, thereby degrading the vessel's hydrodynamic performance. In this study, it is assumed that the ship operates with one year's worth of fouling accumulation. This assumption is justified by typical cruise ship maintenance practices, which include annual hull cleaning and dry-docking every 2 to 3 years for routine maintenance, inspections, and upgrades, depending on the vessel's age, condition, and operational profile. The additional resistance due to fouling is assessed here using an empirical method [110].

Stabilising fins are used on cruise ships to diminish ship roll in rough seas and are typically of the active type, meaning they are deployed when the sea conditions exceed a certain severity threshold. The increase in resistance due to their use is assessed following the methodology proposed in [111] and it is assumed that fins are activated only for sea state 5 or higher, corresponding to significant wave heights H_s greater than 2.5 meters.

Finally, the resistance is adjusted to account for the shallow water effect. When navigating in shallow or restricted water, a ship is affected by an increase in resistance as a function of its speed and submerged size with respect to the water depth. The effect is significant when the ship navigates long sublegs at high speed in shallow waters, typically near the coast, in large estuaries, in port areas or lagoons. This condition, which is called incipient shallow water, is here modelled by introducing a speed loss function of the ship speed and the water depth while keeping the resistance constant [112].

3.2.4 Fuel consumption calculation

For each subleg, once the force equilibrium system is solved, the ship's advance speed (V_A) and propeller thrust (T) can be calculated. These are used to determine the Papmel coefficient, which relates thrust to propeller characteristics. The propeller's operating point is found using corrected performance curves that account for fouling. This allows the calculation of torque and propeller revolution speed, from which brake power is derived. The required electric propulsion power is then calculated, considering efficiencies of the Propulsion Electric Motor (PEM) and its transformers and converters. The total electric demand includes electric demand from propulsion, air conditioning chillers, freshwater production, scrubbers and other auxiliary systems, adjusted by the efficiency of the switchboards, while the remainder constant powers are extracted from the ship's electric balance and aggregated.

In more detail, the propeller functioning point is evaluated from the Papmel coefficient:

$$\left(\frac{K_T}{J^2}\right)^* = \frac{T}{\rho_w V_A^2 D_p^2} \tag{9}$$

where K_T is the propeller thrust coefficient, J is its advance coefficient, D_p is its diameter, and ρ_w the seawater density. After correcting the propeller curves to account for fouling [110], the propeller functioning point J^* is found by interpolation of the $J(K_T/J^2)$ curve corresponding to the Papmel coefficient. Then the absorbed torque Q and revolutions per second n_p of the propeller are calculated as:

$$Q = K_Q(J^*)\rho_w n_p^2 D_p^5 \tag{10}$$

and

$$n_p = \frac{V_A}{J^* D_p} \tag{11}$$

Thus, the brake power, P_B, is:

$$P_B = \frac{2\pi n_p Q}{\eta_R \eta_s} \tag{12}$$

where η_R and η_s are the rotative relative coefficient and the shaft efficiency, respectively. Then, the propulsion electric power, P_{prop}, is determined:

$$P_{prop} = \frac{n_s P_B}{\eta_{PEM}\eta_{tc}} \tag{13}$$

where η_{PEM} is the PEM efficiency evaluated as a function of its load, η_{tc} is the efficiency of the transformers and converters, and n_s is the number of shafts. Finally, the total electric power demand, P_{el}, is calculated as follows:

$$P_{el} = \frac{P_{noaux} + P_{aux}}{\eta_{sw}} \tag{14}$$

with P_{aux} the electric power of the other auxiliary systems, η_{sw} is the efficiency of the switchboards and the non-auxiliaries power P_{noaux} is defined as:

$$P_{noaux} = P_{prop} + P_{ch} + P_{fw} + P_{scrub} + P_{const} \tag{15}$$

where P_{ch} is the electric demand from air conditioning chillers, P_{fw} from freshwater production, P_{scrub} from scrubbers, and P_{const} are the remaining constant powers.

The electric power is generated by multiple diesel generators, so it is necessary to regulate the number and load of the active ones by the Power Management System (PMS). The rules of the PMS regulate the number and the load l_{g_i} of online generators, defined as:

$$l_{g_i} = \frac{P_{el_i}}{\eta_G P_i^{max}} \tag{16}$$

where P_{el_i} is the electric power produced by the *i*-th generator, P_i^{max} is the maximum continuous rating of the engine and η_G is the generator efficiency. The rules adopted in the algorithm are the ones typically employed: all the active generators work at equal load; if the load per generator exceeds or drops below defined thresholds, generators are activated or reactivated, respectively. These rules are modelled through the mapping of the fuel consumption (in t/h) for each type of fuel as a function of the power P_{el}. The global load of the power plant l_g is defined as:

$$l_g = \frac{P_{el}}{P_G} \tag{17}$$

where P_G is the maximum electric power provided by the diesel generators:

$$P_G = \eta_G \sum P_i^{max} \tag{18}$$

Finally, for a configuration, the fuel consumption of the *i*-th engine using the *j*-th type of fuel is calculated as:

$$fc_{i,j} = \sum_i d_j SFOC_{ij}(l_{g_i}) P_i^{max} \, l_{g_i} \tag{19}$$

where d_j is a coefficient accounting for depuration/filtering allowance (equal to 1.015 for HSFO and VLSFO and equal to 1 for MGO), $SFOC_{ij}$ is the specific fuel consumption of the *i*-th engine using the *j*-th fuel at load l_{g_i}.

3.3 Considered fuel types

The selection of fuel scenarios is driven by their current or near-term deployability in the passenger ship sector and by their relevance within existing and forthcoming regulatory frameworks. The objective of the analysis is not to identify a single long-term net-zero solution, but to quantify how different fuel pathways, spanning conventional, transitional, and renewable options, are affected by regulatory mechanisms and operational constraints over the vessel's service life. The calculations are performed using three main fuels: HSFO (reference fuel for business as usual), LNG (widely used transition fuel for passenger ships) and MeOH (possible future fuel for passenger ships). Here, three types of MeOH are considered according to their production process to capture the different impacts on the WtT emissions: NG-MeOH, bio-MeOH and e-MeOH. Additionally, MGO is used as fuel for boilers and as a pilot fuel for dual-fuel engines powered by LNG and MeOH.

3.4 Emission assessment

As the case-study vessel operates on intra-EU routes in the Adriatic Sea, the EU instruments (EU ETS, FuelEU Maritime and CII) constitute the binding and currently enforceable cost drivers and are therefore adopted as the cost basis of this study, whereas the GFI enters into force only from 2028 and remains under negotiation; the methodology, however, is structurally transferable to the IMO Net-Zero Framework once the GFI targets and pricing parameters are finalised. To assess the ship's emission levels for the selected route, the CO_2 equivalent and the GHG and CII indexes are calculated from the fuel consumption fc assessed through Equation (19). The simulation algorithm evaluates the ship's performance for each subleg of the defined route. To calculate the quantity of emissions produced by combustion, the simulation algorithm is provided with the chemical-physical characteristics of each fuel used. Table 2 reports the emissions characteristics of each tested fuel. All the values are taken from the FuelEU regulation [4], with the exception of the CO_2 equivalent WtT factors of bio-MeOH and e-MeOH. For the first, production from biomass obtained from black-liquor gasification integrated with pulp mill was chosen, while the last one is produced via direct air capture of CO_2 and hydrogen from renewable (green or purple) sources, thus making it possible, in agreement with the EU regulations, to fix the CO_2 emission coefficient to zero [64, 113-116]. Regarding LNG, methane slip (C_{slip}) is modelled using the fixed default factors prescribed by the regulatory frameworks, i.e., 3.1 % according to FuelEU Maritime and 3.5 % according to the IMO guidelines, both associated with a Global Warming Potential (GWP) value of 28.

Table 2 Emission coefficients of the fuels tested [4, 47]

Fuel	CO_2eq WtT [g/g$_{fuel}$]	EF CO_2 [g/g$_{fuel}$]	EF CH_4 [g/g$_{fuel}$]	EF N_2O [g/g$_{fuel}$]	C_{slip} [%mass$_{fuel}$]
HSFO	13.5	3.114	0.00005	0.00018	-
MGO	14.4	3.206	0.00005	0.00018	-
LNG	18.5	2.750	0.00	0.00011	3.1
MeOH (natural gas)	31.3	1.375	0.00005	0.00018	-
Bio-MeOH	10.4	0	0.00005	0.00018	-
e-MeOH	4.4	0	0.00005	0.00018	-

These values are adopted to ensure consistency with the regulatory scenarios analysed, acknowledging that methane slip can vary with engine load and operating conditions. This variability is therefore listed as a limitation of the study and should be addressed in future probabilistic analyses. For each subleg (*k*), the grams of fuel consumed in the *i*-th fuel-consuming unit are calculated as:

$$M_{k,i,j} = 10^6 fc_{k,i,j} \frac{D_k}{V_k} \tag{20}$$

and the consumed mass of the *j*-th fuel used:

$$M_{k,j} = \sum_i M_{k,i,j} \tag{21}$$

where $fc_{k,i,j}$ is the fuel consumption of the *j*-th fuel used in the *i*-th fuel-consuming unit in the *k*-th subleg; D_k is the distance covered by the ship in the *k*-th subleg (in nautical miles) and V_k its speed (in knots). To compute the emissions in term of grams of equivalent CO_2, the GWP of the emissions components has to be known. The GWP values for CO_2, CH_4 and N_2O are reported in Table 3 [47].

Table 3 Global Warm Potential of CO_2, CH_4 and N_2O - 20-year and 100-year time-horizon

GWP	CO_2	CH_4	N_2O
GWP20	1	84	264
GWP100	1	28	265

Then, for each subleg (*k*), the algorithm calculates the amount of WtT and TtW emissions [4] as:

$$WtT_k = \frac{\sum_j M_{k,j} LCV_j CO_{2eq,WtT,j}}{\sum_j M_{k,j} LCV_j RWD_j} \tag{22}$$

$$TtW_k = \frac{\sum_j M_{k,j} \left[\left(1 - \frac{C_{slip,j}}{100}\right) CO_{2eq,TtW,j} + \frac{C_{slip,j}}{100} CO_{2eq,TtW,slip,i,j} \right]}{\sum_j M_{k,j} LCV_j RWD_j} \tag{23}$$

where $CO_{2eq,WtT}$ and $C_{slip,j}$ are respectively the CO_2 equivalent WtT emission factor and the carbon slip factor of the *j*-th fuel, as given in Table 2. LCV_j is the low calorific value of the fuel j. and RWD_j is a correction factor equal to 2, applied when the fuel used falls within the European category of RFNBO, and equal to 1 for all other fuel types. Then:

$$CO_{2eq,TtW,j} = EF_{CO_2,j} GWP_{CO_2} + EF_{CH_4,j} GWP_{CH_4} + EF_{N_2O,j} GWP_{N_2O} \tag{24}$$

and

$$CO_{2eq,TtWslip,j} = GWP_{CH_4} \tag{25}$$

The 100-year horizon GWP values are used. Finally, the total emission WtW of the k-th subleg is calculated as the sum of its WtT and TtW emissions:

$$WtW_k = WtT_k + TtW_k \tag{26}$$

The GHG is calculated as in Equation (3), with the wind factor f_{wind} equal to 1, since the cruise ship propulsion is not wind-assisted. However, since the distance travelled varies for each subleg and fuel usage depends on the specific operational phase, it is necessary to separately compute the numerator and denominator of Equations (22) and (23) for the entire journey. The same approach has to be applied for the calculation of the attained CII (CII_A), with some small differences:

$$CII_A = \frac{\sum_k \sum_j M_{k,j} \, EF_{CO_2,j}}{GT \cdot D} \tag{27}$$

where GT is the gross tonnage of the ship. The IMO regulations require that the CII be calculated by considering only CO_2 emissions from combustion, excluding methane slip, upstream emissions, and all other GHG components. This explains why LNG shows a favourable CII despite higher WtW GHG emissions: methane slip and upstream contributions, which are significant for LNG, are excluded from the CII metric but included in the WtW calculation. For reference, methane slip is fixed at 3.1 % according to FuelEU Maritime and at 3.5 % according to IMO guidelines, with a GWP value of 28 [4, 47]. Hence, its contribution is not negligible, and an alternative indicator (CII_A^*) incorporating CO_2-equivalent methane emissions is introduced to illustrate the effect of including methane slip. Here, for comparison purposes, in the case of the LNG configuration, two CIIs are calculated: the one defined in Equation (27) and:

$$CII_A^* = \frac{\sum_k \sum_j M_{k,j} \left[\left(1 - \frac{C_{slip,j}}{100}\right) EF_{CO_2,j} + \frac{C_{slip,j}}{100} GWP_{CH_4} \right]}{GT \cdot D} \tag{28}$$

Although the GHG and CII indicators are defined on an annual basis, the same route is repeated identically multiple times throughout the year. Therefore, the calculation performed for a single voyage is representative of the annual condition. Then, the reference value, CII_R, for a cruise ship is calculated as [11]:

$$CII_R = a \cdot Capacity^{-c} \tag{29}$$

where a, *Capacity* and *c* are parameters function of the ship type. The annually required CII, $CII_{y,R}$, is calculated as [117]:

$$CII_{y,R} = CII_R \left(1 - \frac{Z}{100}\right) \tag{30}$$

where Z is a reduction factor, equal to 0.09 in 2025 and which increases by 0.02 each year until 2026. Finally, for the forecasting, it is assumed that the annual 2 % reduction will also be applied after 2027: in fact, IMO has prescribed to apply the reduction until 2027; from the following year onward, further reductions are yet to be defined [117]. Finally, the yearly ranking is determined as the ratio between CII_A and $CII_{y,R}$, with reference to the threshold values of categories A to E, function of the ship type [12]. Similarly, when the alternative indicator CII_A^* is used, the ratio $CII_A^*/CII_{y,R}$ represents the relative compliance status obtained when methane slip is included in CO_2-equivalent terms. This comparison is provided solely to illustrate the effect of methane slip on the vessel's apparent carbon intensity.

3.5 Energy costs assessment

In addition to costs related to fuel consumption, it is now necessary to apply the EU ETS and account for potential FuelEU penalties. These represent additional costs that, over the years, impact on the ship's energy costs with a variable weight. To analyse their impact over the ship's lifetime, energy costs are calculated from 2025 to 2050, considering a fixed inflation rate of 2% annually - in line with the target set by the European Central Bank [118]. For the Carbon Allowance Cost and fuel prices, taking those from March

2025 as baseline prices [119-122] (see Table 4). This assumption was chosen because the fluctuations of the global market and the geopolitical situation led to different price forecasts with wide ranges of uncertainty, thus not allowing the selection of sufficiently valid values. One exception is the price of e-MeOH, which, according to a forecast [120], decreases from 2,238 €/t to 1,325 €/t between 2025 and 2033 and then remains stable until 2050 (Figure 2).

Table 4 Price of the fuels tested as of March 2025

Fuel	HSFO	MGO	LNG	MeOH	Bio-MeOH	e-MeOH
Price [€/t]	412	656	480	625	1,1193	2,238 (2025) 1,325 (2034)

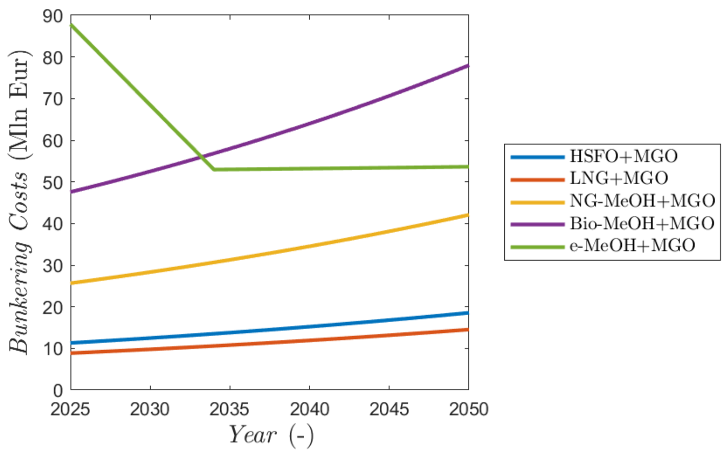

Fig. 2 Bunker costs in 2025-2050 – All fuels

The total energy cost is given by:

$$EC_y = FC_y + ETSC_y + FEUC_y \tag{31}$$

Referring to a given year (y), FC_y (Equation (32)) represents the total cost of consumed fuels and $ETSC_y$ and $FEUC_y$ are calculated as in Equations (34) and (36), respectively. For the bunker costs, it is:

$$FC_y = \sum M_{y,j} P_{j,y} \tag{32}$$

where $M_{y,j}$ is the mass of the j-th fuel, in tons, and $P_{y,j}$ is the price of the fuel, in €/t, taking account of the increase due to inflation as:

$$P_{y,j} = P_{0,j}(1 + 0.02)^y \tag{33}$$

Since the ship operates in the Adriatic Sea and calls at European ports, it must comply with European emission regulations. Therefore, the prescribed Carbon Allowance from the EU ETS (Equation (34)) and the penalties resulting from non-compliance with the FuelEU initiative (Equation (36)) are also calculated [4, 14]. The annual costs associated with the purchase of carbon allowances on EU ETS are calculated as:

$$ETSC_y = n\alpha\beta \sum_k \sum_j M_{k,j} CO_{2eq,WtT,j} CP_y \tag{34}$$

where $CO_{2eq,TtW,j}$ is defined as in Equation (24), $M_{k,j}$ as in Equation (21), α is a coefficient equal to 1 if the ship sails only between European ports, 0.5 if it touches EU and non-EU ports, 0 if it touches only non-EU ports, β is a coefficient equal to 0.7 in 2025 and equal to 1 from 2026 onwards and n is the number of trips in a year. The Carbon Price CP_y is calculated taking into account the interest rate for each year, y:

$$CP_y = CP_0(1 + 0.02)^y \quad (35)$$

Additionally, the EU ETS calculation for 2025 differs from that for subsequent years. Specifically, the regulation mandates that only CO_2 emissions be considered in 2025, while from 2026 onward, CH_2 and N_2O emissions must also be included.

Regarding the FuelEU penalty, if the ship's GHG index, GHG_{ship} (Equation (3)) is major of the target GHG index value $GHG_{target,y}$ (evaluated as the yearly time-dependent percentage of the 2024 limit) the penalty is equal to 0€, otherwise it is calculated as:

$$FEUC_y = \frac{2400|CB_y|}{41000 \cdot GHG_{ship}}\left(1 + \frac{p_y - 1}{10}\right) \quad (36)$$

where p_y is the yearly number of consecutive non-compliance years and CB_y is the compliance balance defined as:

$$CB_y = n\left(GHG_{target,y} - GHG_{ship}\right)\sum_k \sum_j M_{k,j} LCV_j \quad (37)$$

3.6 Sensitivity analysis

To assess the robustness of the economic results presented in Section 5, two independent sensitivity analyses were conducted. The first examines the response of total energy costs to fuel price uncertainty, considering three market scenarios spanning observed price conditions between March 2025 and May 2026. The second addresses the impact of methane slip on the LNG pathway, a parameter whose regulatory default value has been shown to systematically underestimate real operational emissions; three scenarios are defined based on the normative default (FuelEU Maritime, 3.1 %), onboard measurements from a newbuild cruise ship (4.5 %), and fleet-average field measurements (6.4 %).

3.6.1 Fuels prices

To assess the robustness of the economic results under fuel market uncertainty, a sensitivity analysis was conducted on the total energy cost of each fuel pathway. The scenario range spans two price observations recorded in March 2025 and May 2026, bracketing the price variability documented in the maritime fuel market over this period and providing a historically grounded bound for the sensitivity analysis. Three scenarios are defined: S-low (March 2025 prices, baseline), S-mid (arithmetic mean), and S-high (May 2026 prices). For each scenario, the total annual energy cost is decomposed as in Equation (31). For HSFO, MGO, and MeOH, the prices are taken from [119, 122]. For bio-MeOH, the March 2025 market price of 1,193 €/t was used as the baseline, with the scenario range constructed from institutional projections [123]. For e-MeOH, the baseline price profile declines linearly from 2,238 €/t (2025) to 1,325 €/t (2034), remaining constant thereafter [120]. Only the 2025 starting price differs across S-low, S-mid, and S-high. In Table C3 of Appendix C, the fuel prices as of May 2026 are presented. The 2025 baseline value is treated as representative of the 2025–2026 near-term period, consistent with the absence of evidence of significant price reductions in market assessments for e-MeOH as a marine fuel during this timeframe [123]. All other parameters, such as fuel consumption, EU-ETS allowance prices, and FuelEU Maritime penalty factors, are held constant. The price sensitivity is quantified through the arc elasticity of total cost with respect to the main fuel price, computed year-by-year as:

$$E_{fuel} = \frac{\left(EC_{tot,high} - EC_{tot,low}\right)/EC_{tot,mid}}{\left(\overline{p}_{high} - \overline{p}_{low}\right)/\overline{p}_{mid}} \quad (38)$$

where $EC_{tot,high}$ and $EC_{tot,low}$ are the total energy costs under scenarios S-high and S-low respectively, $EC_{tot,mid}$ is the total energy cost under the S-mid scenario used as normalisation reference, and $\overline{p}_{high}$, $\overline{p}_{low}$,

$\overline{p}_{mid}$ are the corresponding main fuel prices defining the scenario range. For e-MeOH, the three scenarios share the same linear decline trajectory and the same floor price of 1,325 €/t from 2034 onward; only the 2025 starting price differs across S-low, S-mid, and S-high, producing three parallel price profiles that converge to an identical value from 2034. The arc elasticity is therefore defined exclusively over 2025-2033, the interval during which the scenarios are distinguishable. For fuel pathways involving auxiliary MGO consumption alongside the main fuel, the normalising price variable $\overline{p}$ in Equation (37) refers exclusively to the main fuel. MGO price is varied across scenarios proportionally and consistently, but its contribution enters only through EC_{tot}. The elasticity is thus interpreted as the sensitivity of total energy cost to the main fuel price, with auxiliary fuel price variation treated as a correlated covariate rather than an independent parameter.

3.6.1 Methane slip

The sensitivity analysis adopts methane slip as the independent variable, defined as the fraction of LNG mass escaping unburned as CH4 during combustion. It is well established that large cruise ships rely almost exclusively on low-pressure dual-fuel four-stroke (LPDF 4-S) medium-speed engines; the analysis is restricted to this technology class. Three scenarios are defined: S_1, with a slip of 3.1 %, adopts the regulatory default of FuelEU Maritime Regulation [4]; S_2, with a slip of 4.5 %, is derived from onboard measurements conducted on a newbuild cruise ship [124]; S_3, with a slip of 6.4 %, corresponds to the fleet average from 22 plume measurements on 18 vessels, the value recommended by ICCT as the revised default for LPDF 4-S engines [125]. For each scenario, the total annual energy cost is decomposed as in Equation (31). Sensitivity is quantified through the arc elasticity of the energy costs with respect to the slip coefficient:

$$E_{slip} = \frac{\left(EC_{S_3} - EC_{S_1}\right)/\overline{EC}}{\left(C_{slip,S_3} - C_{slip,S_1}\right)/\overline{C}_{slip}} \tag{39}$$

where EC_{S_3} and EC_{S_1} are the total annual energy costs under scenarios S_1 and S_3 for each year, $\overline{EC}$ is the energy costs arithmetic mean among the scenarios, used as the normalisation base to obtain a dimensionless relative cost variation. C_{slip,S_3} and C_{slip,S_1} are are the methane slip values of the high and low extremes and $\overline{C}_{slip}$ is the methane slip coefficients arithmetic mean of the among the scenarios. The ratio E_{slip} therefore measures the percentage change in total energy cost per unit percentage change in methane slip, evaluated between the two bounding scenarios and normalised at their midpoint. The arc elasticity formulation is retained for consistency with the companion fuel-price sensitivity analysis. Since C_{slip} is a technology-fixed parameter rather than a time-varying market variable, the denominator is constant; temporal variations in E_{slip} therefore isolate the evolution of the cost structure (specifically, the growing dominance of the FuelEU penalty) as the sole driver of changing sensitivity.

4. Application

In this section, the application of the proposed methodology to an Adriatic cruise repeated for one year is presented. After defining the itinerary, the test ship characteristics, the propulsive configurations, and the environmental data sources are provided, focusing on three different fuels: HSFO, LNG, and MeOH.

4.1 Itinerary

The itinerary chosen for this study (Figure 3) covers three ports in the Adriatic Sea, with a duration of three days. The port calls are Venice (ITVCE), Koper (SIKOP), and Zara (HRZAD), concluding with a return to Venice (ITVCE). The trip duration is 72 h (three days), of which 59.6 % in navigation, 38.1 % in port stay, and 2.3 % in transit and manoeuvring. For the annual calculations, the voyage is repeated 116 times in a year. The detailed schedule and discretisation of the itinerary are reported in Appendix A.

Fig. 3 Ship's itinerary

4.2 Tests Ship

The simulations were carried out on a cruise vessel, whose main characteristics are shown in Table 5. The fuel storage system has been adapted to accommodate the specific requirements of each fuel tested. The fuel tanks' capacity for each configuration is reported in Table 6, together with the genset configuration. HSFO, LNG, and MeOH each require distinct storage solutions due to their differing physical-chemical properties. The vessel was originally designed for conventional diesel fuel, featuring structural tanks suitable for HSFO and MGO bunkering. This configuration has been used as the baseline case and is referred to as the "Diesel" ship. Also, LNG and MeOH require a different kind of engine, referred to as "dual-fuel", which can run on both gaseous and liquid fuels. In Table 6, the dual-fuel engines are identified by the acronym "DF" in the name, while the engines burning liquid fuels only are identified by "F".

Table 5 Main Characteristics of the test ships

Dimension	**ID**	**Value**	**Unit**	**Dimension**	**ID**	**Value**	**Unit**
Length Overall	L_{OA}	330.00	m	Pitch-Diameter Ratio	PD	1.10	-
Length between Perpendicular	L_{PP}	311.00	m	Expanded Area Ratio	A_E/A_0	0.57	-
Design Beam	B	43.20	m	Number of generators	-	4	-
Design Draft	T	8.35	m	Propulsion Electric Motors Power	P_{PEM}	2x20,000	kW
Gross Tonnage	GT	181,500	GT	Auxiliaries Power	P_{aux}	9,100	kW
Number of propellers	-	2	-	Hotel Power	P_{hotel}	531,00	kW
Propeller Diameter	D	6.10	m	Chiller Power	P_{ch}	12,500	kW
Number of Blades	Z	5	-	Maximum Passengers number Maximum Crew members number	-	6,340 1,700	-

Table 6 Fuels and gensets configurations

Characteristics	**"Diesel"**	**"LNG"**	**"MeOH"**	**Unit**
Main Fuel Tanks Capacity	3,301.6	3,699.9	2,986.0	m^3
MGO Tanks Capacity	955.5	2,808.3	955.5	m^3
2x Father Diesel Genset	Wärtsilä 16V46F	Wärtsilä 16V46DF	Wärtsilä 16V46DF	-
2x Son Diesel Genset	Wärtsilä 12V46F	Wärtsilä 12V46DF	Wärtsilä 12V46DF	-

The LNG-fuelled variant is equipped with bilobed cylindrical tanks, and its internal arrangement was developed to ensure a feasible and safe integration within the existing hull structure [45], although subdivision has been modified to meet the rule requirements applicable to LNG fuel [85]. The MeOH-fuelled variant requires comparatively minimal retrofitting, as MeOH can be stored in conventional structural tanks provided that cofferdams are installed for isolation. This configuration is therefore similar to the original diesel-fuelled design, with the tank capacity reduced to account for the volume occupied by the cofferdams. Unlike fossil fuels and LNG, MeOH can be safely stored in tanks located along the hull shell below the vessel's minimum operational waterline. Hence, additional MeOH tanks were installed in the double bottom beneath the main fuel tanks to improve the ship's range. The propulsion system of the ship is diesel-electric, composed of 2 PEMs having a maximum power of 21 MW each. The calm water resistance is provided in Figure 4, and the propeller open water diagram is depicted in Figure 5. The onboard power plant comprises 4 diesel generators arranged in a father-son configuration (Table 7) producing 62,400 kW, having an efficiency η_G of 0.97. Fuel consumption in ISO conditions, considering an even load PMS, is reported in Figure 6, while the pilot-fuel consumption (specifically, MGO) of the dual-fuel engines configuration is depicted in Figure 7 [126, 127]. The electric distribution system has a switchboard efficiency η_{SB} of 0.999, while the transformers and converters of the propulsion system have, respectively, an efficiency η_{Tran} of 0.99 and η_{Conv} of 0.985.

Table 7 Characteristics of the test ship's generators

Model	Type	Allowed Fuel	P_{min} (kW)	P_{max} (kW)
Wärtsilä 12V46DF	Diesel Genset	MGO/HSFO/LNG/MeOH	2,880	14,400
Wärtsilä 16V46DF	Diesel Genset	MGO/HSFO/LNG/MeOH	3,360	16,800
Wärtsilä 12V46F	Diesel Genset	MGO/HSFO	2,880	14,400
Wärtsilä 16V46F	Diesel Genset	MGO/HSFO	3,360	16,800

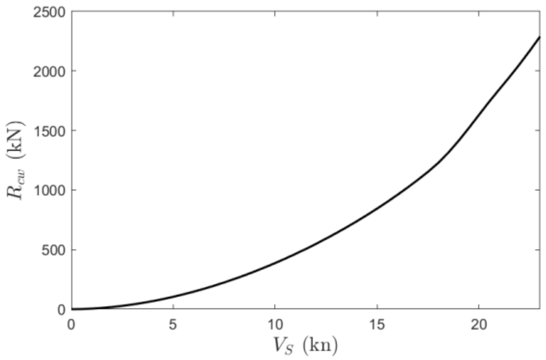

Fig. 4 Total Resistance curve in calm water of the test ship

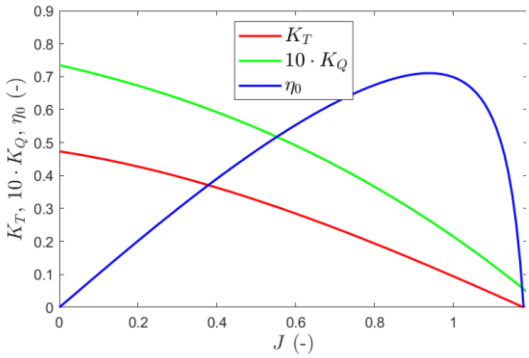

Fig. 5 Propeller open water diagram

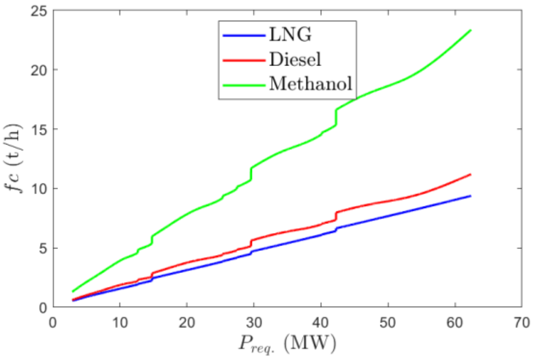

Fig. 6 Fuel consumption according to even load PMS – Main fuel (HSFO, LNG, MeOH)

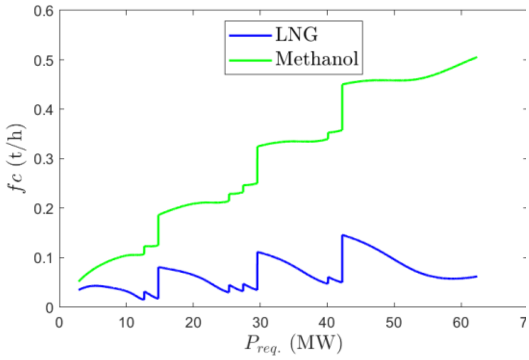

Fig. 7 Fuel consumption according to even load PMS – Pilot fuel (MGO)

4.3 Environmental conditions in the Adriatic Sea

The annual average current speed is calculated by extracting the monthly average currents from the North Atlantic pilot charts, which cover the Mediterranean Sea and, thus, the Adriatic Sea [105]. The average value of the current speed is equal to 0.225 knots, with direction as in the Pilot Charts (which does not change much during the year for the Adriatic Sea). The annual statistics on significant wave height, zero-period crossing, and wind speed for the entire Adriatic Sea are used [106]. The annual average wind speed is equal to 5.37 knots. The statistics for the entire Adriatic Sea were used as given in Figures 8 and 9 and the computed value of the average wave added resistance is given against ship speed in Figure 10.

T_p/H_s	0.0–0.5	0.5–1.0	1.0–1.5	1.5–2.0	2.0–2.5	2.5–3.0	3.0–3.5	3.5–4.0	4.0–4.5	4.5–5.0	5.0–5.5	5.5–6.0	6.0–6.5	Sum
0–1	0	0	0	0	0	0	0	0	0	0	0	0	0	0
1–2	0	0	0	0	0	0	0	0	0	0	0	0	0	0
2–3	221,186	65,034	754	7	0	0	0	0	0	0	0	0	0	286,981
3–4	149,331	225,790	32,459	1233	39	1	1	0	0	0	0	0	0	408,854
4–5	36,859	130,876	80,830	19,669	1732	109	7	1	0	0	0	0	0	270,083
5–6	17,747	52,597	54,473	38,089	15,605	3194	469	54	3	0	0	0	0	182,231
6–7	10,379	24,193	20,917	17,297	14,389	8836	3255	731	183	32	5	2	1	100,220
7–8	3704	8591	8993	6373	4838	3810	3141	1879	701	215	54	18	10	42,327
8–9	1863	3459	3515	2727	1930	1361	956	677	470	197	78	13	8	17,254
9–10	1174	1055	1115	819	654	495	336	231	156	92	48	26	3	6204
10–11	376	434	420	294	217	120	98	64	40	22	6	2	1	2094
11–12	363	105	107	81	91	31	26	16	10	9	5	2	1	847
12–13	434	39	23	10	8	10	7	7	2	2	1	1	0	544
13–14	0	0	0	0	0	0	0	0	0	0	0	0	0	0
Sum	443,416	512,173	203,606	86,599	39,503	17,967	8296	3660	1565	569	197	64	24	1,317,639

Note. Total of 73% of sea states are less than 1 m.

Fig. 8 Sea state table - Entire Adriatic Sea [106]

u_w/H_s	0–0.25	0.25–0.5	0.5–0.75	0.75–1	1–1.25	1.25–1.5	1.5–1.75	1.75–2	2–2.25	2.25–2.5	2.5–2.75	2.75–3	3–3.25	3.25–3.5	Sum
0–1	20,070	33,291	10,955	3152	1198	462	187	81	29	26	4	3	1	0	69,459
1–2	32,250	68,242	25,570	7861	2803	1134	453	200	83	23	9	7	2	2	138,639
2–3	27,155	84,153	38,583	12,391	4471	1707	703	313	131	61	23	17	5	3	169,716
3–4	14,064	81,193	52,240	18,013	6548	2608	1067	437	209	86	47	24	7	9	176,552
4–5	5139	54,153	66,294	24,730	9238	3666	1504	614	306	104	70	23	26	8	165,875
5–6	1666	16,761	68,671	35,231	12,912	5099	2161	990	425	209	90	48	16	6	144,285
6–7	393	3321	37,421	45,709	18,845	7541	3211	1419	628	295	132	63	38	17	119,033
7–8	103	964	8754	37,098	26,470	11,372	4919	2082	954	452	232	97	39	26	93,562
8–9	33	310	1519	13,596	25,426	16,301	7712	3415	1534	731	317	160	57	30	71,141
9–10	11	77	416	2830	12,104	16,639	10,722	5572	2490	1196	502	235	96	75	52,965
10–11	6	23	129	625	3206	8879	10,611	7563	3966	1962	815	426	175	112	38,498
11–12	4	16	44	168	770	2781	5704	6793	5306	3051	1556	700	328	155	27,376
12–13	0	10	33	51	161	779	1995	3477	4147	3606	2245	1206	585	249	18,544
13–14	0	6	9	31	66	207	585	1191	2063	2588	2283	1684	975	545	12,233
14–15	0	2	8	15	28	88	192	397	709	1194	1425	1365	1087	698	7208
15–16	0	0	4	9	11	32	69	141	243	398	604	724	823	709	3767
Sum	100,894	342,522	310,650	201,510	124,257	79,295	51,795	34,685	23,223	15,982	10,354	6782	4260	2644	13,088

Fig. 9 Wind speed-significant wave height occurrence table - Entire Adriatic Sea [106]

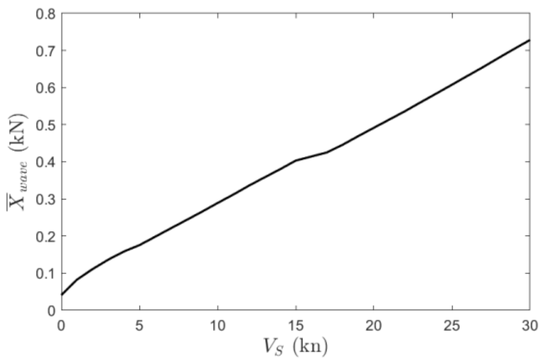

Fig. 10 Average added wave resistance in function of ship speed

5. Results and Discussion

In this section, for each fuel used, the results are presented. In particular, the data on consumption, emissions, and costs, are discussed. Then, the three configurations are compared, highlighting the differences and advantages/disadvantages that emerge from each fuel tested.

5.1 Diesel

In the “Diesel” configuration, the vessel consumes 120.71 tonnes of HSFO and 63.45 tonnes of MGO per voyage, corresponding to an annual consumption of 14,002 tonnes and 7,360 tonnes, respectively. During the navigation phase of a single trip, three engines are operated with an average thermal efficiency of 66.5 %. Each voyage results in TtW GHG emissions amounting to 588.34 tonnes of CO_2 equivalent (CO_2eq), yielding an annual total of 68,247 tonnes. The emissions are primarily composed of CO_2 (98.46 %), with minor contributions from N_2O (1.49 %) and CH_4 (0.17 %). The associated WtT CO_2eq emissions are 105.00 tonnes per voyage and 12,180 tonnes annually. The resulting WtW GHG intensity is 91.3 gCO_2eq/MJ, which exceeds the regulatory limits set by FuelEU Maritime for vessels operating from 2025 onwards. Consequently, a compliance penalty will be applied to the ship's energy costs starting in 2025. In the absence of corrective measures, the penalty will increase by a factor of 148 over 25 consecutive years of non-compliance (refer to Equation (36)). The evolution of GHG intensity and FuelEU compliance for the Diesel configuration is illustrated in Figure 11a.

Regarding the CII, the vessel's reference value is 9.00, while the calculated attained value is 6.97. As a result, the ship is rated in Category "A" for the year 2025. However, without corrective measures, it is projected to become non-compliant by 2036, receiving a "D" rating for two consecutive years, followed by an "E" rating in 2038. In accordance with regulatory requirements, a corrective action plan must be implemented in 2038 to restore the vessel's rating to at least Category "C". The projected CII trend without any corrective action is shown in Figure 11b.

The time evolution of energy costs is illustrated in Figure 11c, while the distribution of cost components over time is shown in Figure 11d. Assuming that EU ETS allowance costs increase solely in line with the inflation rate, their value rises approximately 2.5-fold, from over €3 million in 2025 to around €7.6 million by 2050. In 2025, the distribution of energy costs per voyage is as follows: 71.22 % from fuel bunkering, 21.49 % from EU ETS allowances, and 7.29 % from FuelEU Maritime penalties. Both bunkering and EU ETS costs are assumed to grow at the inflation rate over time. However, their relative shares decline as the FuelEU penalty increases significantly, particularly in 2040, 2045, and 2050, coinciding with progressively stricter GHG reduction targets that worsen the ship's compliance status. By 2050, the FuelEU penalty constitutes the largest share of energy costs (85.25 %), followed by bunkering (10.26 %) and EU ETS allowances (4.49 %). Over the 25-year period, total energy costs escalated from approximately €15 million to €169 million (an increase of more than 11-fold), primarily driven by the FuelEU non-compliance penalty. In contrast, if the penalty were excluded, the total cost increase would be limited to approximately 1.8 times, attributed solely to inflation.

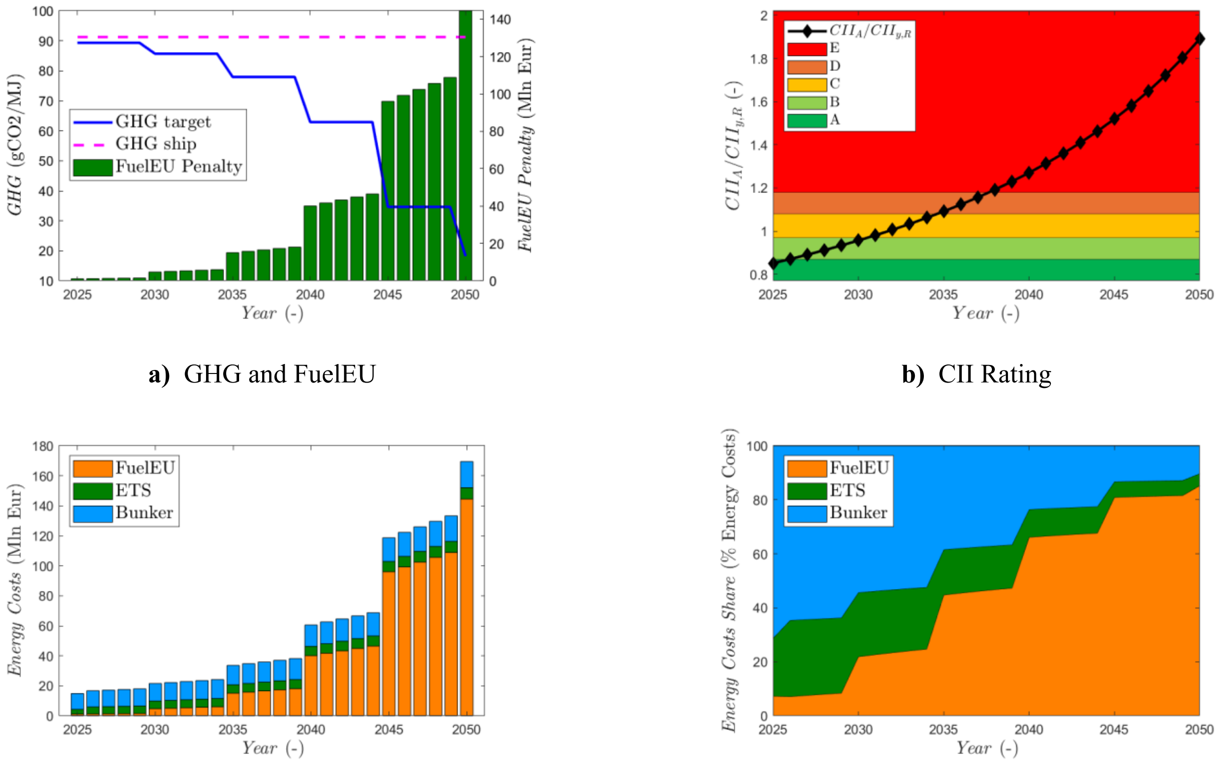

a) GHG and FuelEU

b) CII Rating

c) Energy costs

d) Energy costs shares

Fig. 11 Diesel configuration evolution in 2025-2050

5.2 LNG

In the “LNG” configuration, the vessel consumes 139.26 tonnes of liquefied natural gas (LNG) and 14.13 tonnes of marine gas oil (MGO) per voyage, corresponding to an annual consumption of 16,155 tonnes and 1,639 tonnes, respectively. During the navigation phase of each trip, four engines are operated with an average thermal efficiency of 69 %. The TtW GHG emissions per voyage amount to approximately 541.90 tonnes of CO_2 equivalent (CO_2eq), resulting in an annual total of 62,860 tonnes. While the majority of emissions are due to CO_2 (76.84 %), methane slip contributes significantly (22.31 %), followed by minor contributions from N_2O (0.85 %) and CH_4 (0.03 %). Additionally, WtT emissions are estimated at 135.18 tonnes CO_2eq per voyage, leading to a yearly total of 15,681 tonnes. The resulting WtW GHG intensity is 90.99 gCO_2eq/MJ, which exceeds the FuelEU Maritime compliance threshold already in effect from 2024. Consequently, a FuelEU non-compliance penalty is applied throughout the vessel’s operational life, amounting to approximately €0.9 million in 2025 and rising to around €141 million by 2050. The projected evolution of GHG intensity and FuelEU-related penalties for the LNG configuration is illustrated in Figure 12a.

Concerning the CII, the vessel’s reference value is still 9.00, while the attained value is 5.16. This places the ship in Category “A” from 2025 through 2037. Beginning in 2046, the vessel is projected to fall into Category “E”, rendering it non-compliant with CII regulations. As a result, a corrective action plan must be implemented by 2045 to restore compliance, achieving a rating of at least Category “C”. The projected CII trajectory is illustrated in Figure 12b. It is noteworthy that the CII calculation takes into account only the CO_2 produced by combustion and not the CO_2 equivalent including methane slip, CH_4 and N_2O emissions. Considering the contribution of methane slip (Equation (28)), the CII* value and the ship ranking change substantially: the attained value is 6.48 and the ship is rated in Category “A” only from 2025 to 2029, projected to fall in Category “E” by 2040 (Figure 12b) with a substantial anticipation of the need for corrective actions.

In 2025, the distribution of energy-related costs per voyage is as follows: 69.44 % for bunkering, 23.33 % for EU ETS, and 7.24 % attributed to the FuelEU penalty. Over time, the shares associated with bunkering and EU ETS increase solely due to inflation. By 2050, as observed in the "Diesel" configuration, the FuelEU penalty becomes the dominant component of energy costs in the LNG scenario as well, accounting for 86.81 %, followed by bunkering at 8.89 % and EU ETS at 4.30 %. Over the 25-year period, total energy costs rose from approximately €12.7 million to nearly €163 million (an almost 12-fold increase), primarily driven by the escalating FuelEU penalty. In the absence of this penalty, the cost escalation would be limited to a factor of approximately 1.7, driven solely by inflation. The temporal evolution of total energy costs is presented in Figure 12c, while the breakdown of cost components is shown in Figure 12d.

5.3 Methanol

In the MeOH configuration, the vessel consumes 332.46 tonnes of MeOH and 19.91 tonnes of MGO per voyage, corresponding to annual consumptions of approximately 38,565 tonnes and 2,309 tonnes, respectively. During the navigation phase, the ship operates three engines with a combined average efficiency of 69 %. As previously discussed, three MeOH types are evaluated, differentiated by their production pathways: NG-MeOH, bio-MeOH and e-MeOH.

For the NG-MeOH scenario, each voyage results in approximately 538.26 tonnes of CO_2eq TtW emissions, amounting to 62,438 tonnes annually. These emissions are primarily composed of CO_2 (96.79 %), with minor contributions from N_2O (3.12 %) and CH_4 (0.09 %). In contrast, for bio- and e-MeOH, classified as a renewable biological and non-biological fuel, respectively, TtW emissions are much lower: 81.13 tonnes for each voyage, 9,411 annually (an 84.9 % reduction). This is possible in agreement with the EU regulations, which permit fixing the CO_2 emission coefficient to zero, as the bio-MeOH is produced from biomass (black-liquor gasification integrated with pulp mill) and e-MeOH via direct air capture of CO_2 and hydrogen from renewable (green or purple) sources [64, 113-115].

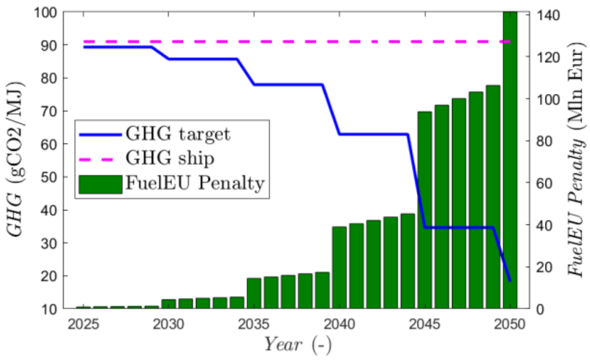

a) GHG and FuelEU

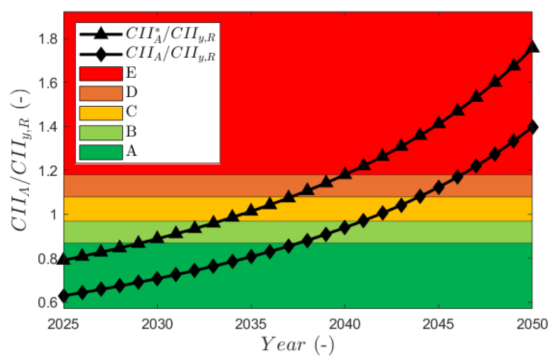

b) CII Rating

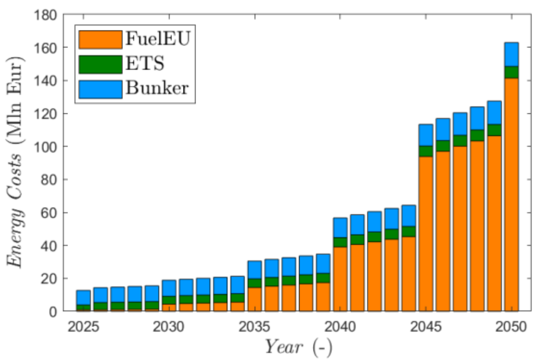

c) Energy costs

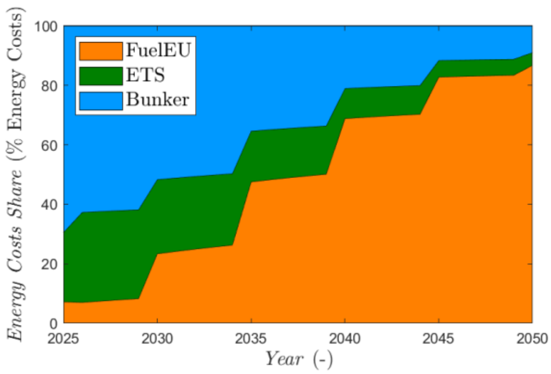

d) Energy costs shares

Fig. 12 LNG configuration evolution in 2025-2050

Consequently, for these cases, the main emission contribution is given by MGO pilot fuel (79.9 % of the total emissions). It is noteworthy that, despite the zero TtW CO_2 emissions allowed by the EU regulations, the configuration using bio-MeOH is not compliant with the FuelEU regulation for the entire period considered, for which the penalty will start to be paid in 2050.

The WtT CO_2eq emissions vary significantly by MeOH type: NG-MeOH results in 219.32 tonnes of WtT CO_2 per voyage, while bio-MeOH yields 81.04 tonnes (a 63 % reduction), and e-MeOH only 41.35 tonnes (an 81.1 % reduction). These values have a direct and substantial impact on the overall WtW GHG emissions and, consequently, on the FuelEU Maritime penalty. In the NG-MeOH case, the GHG WtW intensity reaches 101.47 gCO_2/MJ, exceeding the IMO reference threshold; the vessel is therefore non-compliant even at present, and the FuelEU penalty becomes increasingly significant over time. With bio-MeOH, the GHG WtW value is 21.72 gCO_2/MJ, allowing compliance until 2049, and the FuelEU penalty applies from 2050. In the case of e-MeOH, the GHG WtW intensity—calculated according to the RFNBO framework—is 7.11 gCO_2/MJ from 2025 to 2033 and 14.22 gCO_2/MJ from 2034 to 2050, ensuring compliance throughout the entire regulatory horizon. The temporal evolution of GHG emissions and the associated FuelEU penalties for the three MeOH types is illustrated in Figures 13a, 13b, and 13c. The jump in 2035 of the GHG value for the e-MeOH configuration (Figure 13c) is due to the application of the RWD factor equal to 2, since e-MeOH falls within the European category of RFNBO.

The CII reference value remains constant at 9.00. The calculated CII value is 6.27 for NG-MeOH, placing the vessel in Category “A” from 2025 through 2029. However, beginning in 2038, the vessel becomes non-compliant, having fallen into Category “D” for three consecutive years, in violation of regulatory thresholds. In contrast, when operating with bio- and e-MeOH, the calculated CII is significantly lower at 0.77, ensuring classification in Category “A” through 2050 and full compliance throughout the regulatory period. The progression of CII values over time for the different MeOH types is summarised in Figure 13d.

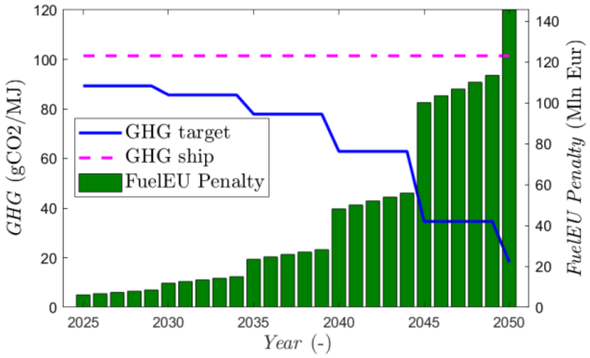

a) GHG and FuelEU – NG-MeOH configuration

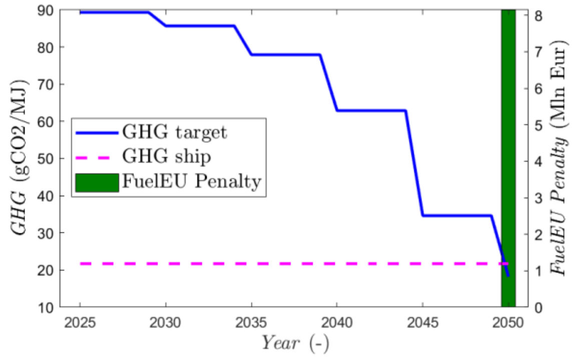

b) GHG and FuelEU – Bio-MeOH configuration

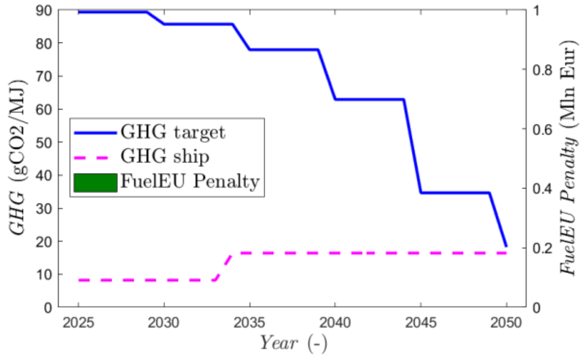

c) GHG and FuelEU – e-MeOH configuration

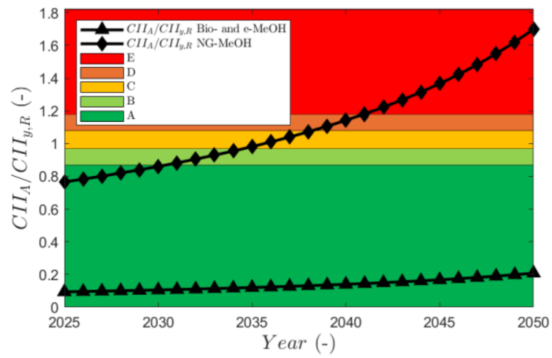

d) CII Rating – MeOH configurations

Fig. 13 MeOH configurations evolution in 2025-2050

Energy costs, which are strongly influenced by the FuelEU penalty, vary significantly depending on the MeOH production pathway. For NG-MeOH, in 2025, 74.13 % of energy costs are attributed to bunkering, 17.54 % to the FuelEU penalty, and 8.32% to EU ETS. By 2050, assuming the vessel remains non-compliant with GHG intensity regulations throughout the period, the FuelEU component becomes dominant, accounting for 74.82 % of total energy costs. Over the 25-year period, energy costs rose from approximately €34.5 million to €194 million. For bio-MeOH and e-MeOH, the cost distribution in 2025 is heavily weighted towards bunkering, which accounts for 99.26 % and 99.60 % of total energy costs, respectively. The remaining shares are due to EU ETS: 0.74 % for bio-MeOH and 0.40 % for e-MeOH. By 2050, bunkering represents the largest cost component for bio-MeOH (89.4 %), followed by FuelEU penalty (9.35 %) and EU ETS (1.20 %). For e-MeOH, the FuelEU penalty remains at 0.00 %, while bunkering and EU ETS contribute 98.08 % and 1.92 %, respectively. Total energy costs over the 25-year period increase from approximately €47 million to €162 million for bio-MeOH, while for e-MeOH, they decrease from €88 million to about €54 million, due to the absence of the FuelEU penalty and lower projected fuel prices. The time evolution of energy costs and their component breakdowns for each MeOH type are illustrated in Figures 14, 15 and 16.

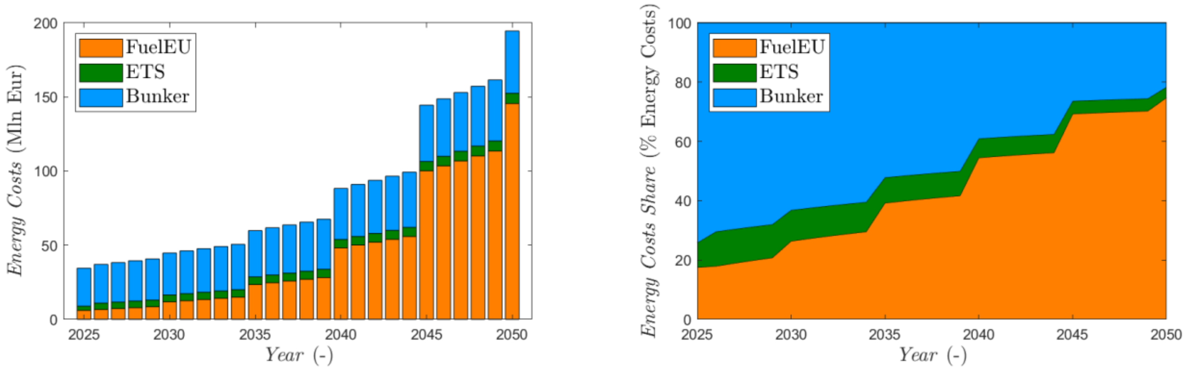

a) Energy costs **b)** Energy costs shares

Fig. 14 Energy costs and shares evolution in 2025-2050 – NG-MeOH configuration

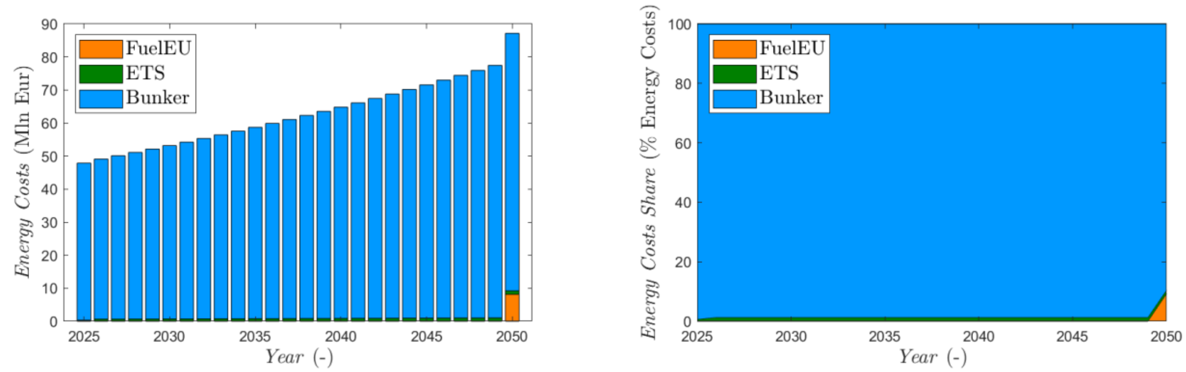

a) Energy costs **b)** Energy costs shares

Fig. 15 Energy costs and shares evolution in 2025-2050 – Bio-MeOH configuration

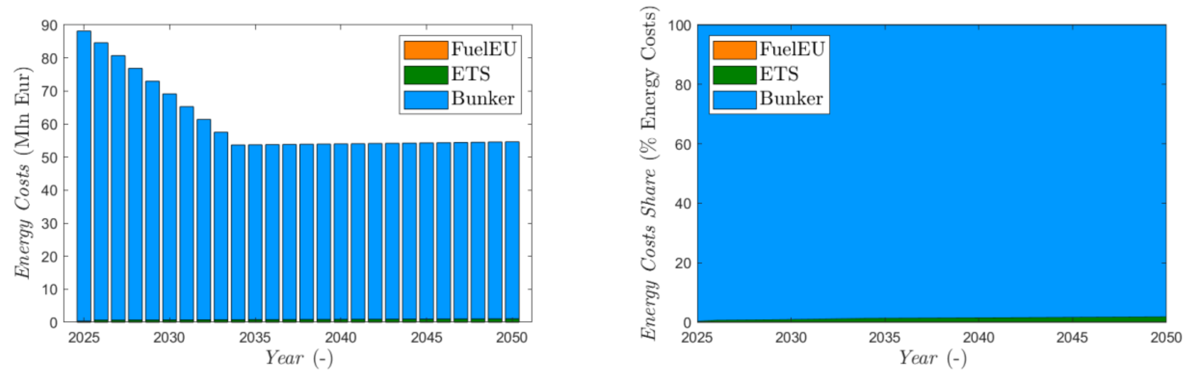

a) Energy costs **b)** Energy costs shares

Fig. 16 Energy costs and shares evolution in 2025-2050 – e-MeOH configuration

5.4 Comparison of the different configurations

Table 8 presents the fuel consumption for a single trip for each fuel type used, along with the corresponding CO_2 equivalent WtW emissions. The fuel that produces the highest amount of emissions is NG-MeOH, which is notably more polluting than the business-as-usual scenario employing HSFO. This is primarily due to the WtT contribution (the highest among all the tested fuels) since the entire production chain is associated with significant emission levels. Nonetheless, the Diesel configuration is still the second most polluting, followed by LNG, bio-MeOH and, finally, e-MeOH. When examining the emissions coming from the analysed types of MeOH, the reduction in emissions occurs primarily in the TtW amount, since they account only for the emissions related to pilot fuel due to the renewable source of bio- and e-MeOH. Besides, the WtT emissions are remarkably reduced when employing bio- and e-MeOH, due to the higher sustainability of the production process. However, since MDO is utilised as pilot fuel, the TtW share remains the most significant in terms of emissions for all fuels, representing 84.85 % for the Diesel configuration, 80.03 % for LNG, 71.05 % for MeOH, 50.03 % for bio-MeOH, and 66.24 % for e-MeOH. Except for bio- and e-MeOH, the primary fuel is responsible for the largest share of overall WtW emissions (Table 9).

Table 8 Fuel consumption and emissions (one voyage)

Configuration	**Diesel**		**LNG**		**MeOH**		
Fuel	HSFO	MGO	LNG	MGO	MeOH	MGO	Type
Tons [t]	120.71	63.45	139.26	14.13	332.46	19.91	-
Volume [m^3]	123.17	71.29	302.75	15.87	444.46	22.37	-
CO_{2eq} WtW [t]	693.35		677.08		757.58		NG-MeOH
					162.18		Bio-MeOH
					122.48		e-MOH

Table 9 WtT, TtW emissions and GHG Emissions Rating for fuel configuration.

Configuration	**Diesel**		**LNG**		**MeOH**		
-	WtT [t]	TtW [t]	WtT [t]	TtW [t]	WtT [t]	TtW [t]	Type
CO_{2eq} [t]	105.00	588.34	135.18	541.90	219.32	538.25	NG-MeOH
					81.04	81.13	Bio-MeOH
					41.35	81.13	e-MeOH
GHG	91.3		90.99		101.47		NG-MeOH
					21.72		Bio-MeOH
					8,20 (until 2033); 16.41		e-MeOH

Regarding the CII, the values calculated for the different configurations are shown in Figure 17 and Table 10. The use of bio- and e-MeOH represents the most favourable option, as the vessel remains compliant with GHG intensity limits over the entire 25-year horizon, with a substantial margin. This compliance buffer would likely accommodate the introduction of more stringent reduction targets beyond 2027, assumed to decrease annually by 2 % until 2050. By contrast, the NG-MeOH configuration would require corrective measures by 2040 to maintain compliance. After bio- and e-MeOH, the LNG configuration (not considering the effects of the methane slip) is the best: it would necessitate intervention only by 2045. However, if emissions related to methane slip are also taken into account (CII*, see Equation (28)), the situation turns upside down, with an index value between those of NG-MeOH and HSFO. In the graph, the relative curve is not visible as it is almost coincident with the NG-MeOH one. The difference in the amount of emissions used for the calculation of the CII and CII* is equal to 109.7 tonnes, corresponding to a 25 % increase. These numbers clearly highlight that the IMO's current rules unjustly favour the use of LNG, not considering all the pollutants in the determination of the CII.

Table 10 CII evolution for fuel configuration

-	CII ship	Compliant	Non-compliant (without corrective intervention)
Diesel	6.97	2025-2036	From 2037
LNG	5.16 (CII) 6.47 (CII)	2025-2045 2025-2038	From 2046 From 2039
MeOH	0.77 6.27	2025-2050 (bio- and e-MeOH) 2025-2039 (NG-MeOH)	Never From 2040

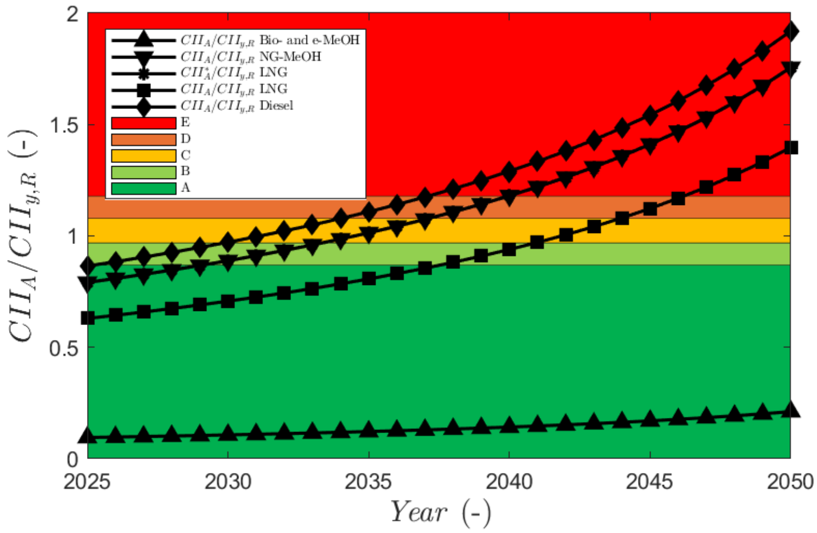

Fig. 17 CII Rating in 2025-2050 – All fuels

On the other hand, the formulas for the GHG calculation and EU ETS, including all the emission components (as for the EU regulations), show almost no advantage of LNG over HSFO. Finally, the Diesel configuration has the worst performance, remaining compliant until 2037. Therefore, under the assumption of a 25-year service life, all options except bio- and e-MeOH (and LNG *de iure*) would require emissions mitigation strategies before mid-life to ensure regulatory compliance.

From a cost perspective, the magnitude of the FuelEU penalty—directly linked to the amount of WtW emissions—emerges as the primary driver of projected energy costs in most analysed scenarios. Taking the Diesel configuration as a reference for the 25-year projection, over the entire period, the use of LNG results in a saving of about €26 million (-2.64 %). Regarding MeOH, if it is produced from natural gas, the expenditure increases by €183.5 million (+18.56 %), whereas the use of bio-MeOH and e-MeOH results in savings of €980 million (-99.17 %) and €989 million (-100 %), respectively. The year-by-year comparison is shown in Figure B1. So, the only configuration that is compliant with the FuelEU Regulation for the entire time period considered is the e-MeOH one.

Regarding the EU ETS, the highest costs are associated with HSFO, followed by NG-MeOH, LNG, bio- and e-MeOH over the entire considered period. This follows directly from the TtW emissions levels, which are only subject to EU ETS obligations. The year-by-year comparison is provided in Figure B2.

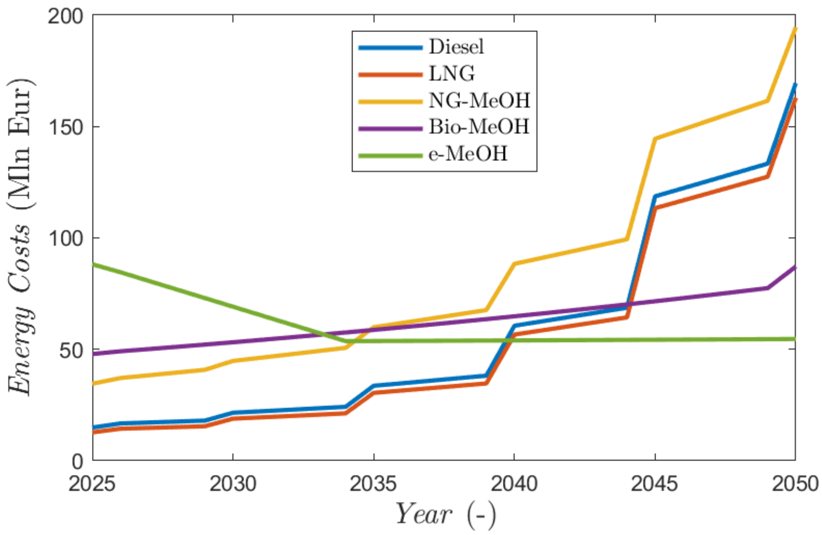

Fig. 18 Energy costs in 2025-2050 – All fuels

Finally, over a 25-year period, the main contributors to energy-related costs are the FuelEU penalty and, obviously, the fuel price (Figure 18). In 2025, the cost-effectiveness of each fuel is primarily determined by its market price, with HSFO and LNG being the most advantageous options. In the following years, the two lose progressively competitiveness due to the increasing FuelEU penalties applied. By 2040, for the analysed cruise itinerary, the most cost-effective option is expected to be the e-MeOH, which is not subject to penalties, as it overtakes HSFO and LNG. NG-MeOH is the least competitive due to its relatively high initial cost and, more significantly, the high FuelEU penalties imposed throughout the vessel's operational life. Finally, on the studied itinerary, bio-MeOH is more competitive than NG-MeOH by 2034 and then HSFO and LNG by 2044, thanks to its minor environmental impact.

5.5 Sensitivity analysis

The results of the two sensitivity analyses are presented below. For each analysis, a discussion on total energy costs, regulatory cost shares, and arc elasticity are reported. The two analyses are complementary: the fuel price sensitivity quantifies the exposure of each pathway to market volatility, while the methane slip sensitivity isolates the regulatory and economic consequences of adopting different emission accounting assumptions for LNG-fuelled vessels. Tables and figures summarizing the results are reported in Appendix C.

5.5.1 Fuel prices

Regarding the energy costs, the results show that total annual energy costs for conventional pathways (HSFO, LNG, MeOH) vary by 23-39 % between S-low and S-high in 2025 (HSFO: €15.6 million to €21.7 million; LNG: €13.8 million to €17.0 million; MeOH: €34.6 million to €43.8 million), with cost variation consistently lower than the fuel price spread due to the buffering effect of fixed regulatory components. The regulatory share (ETS plus FuelEU) ranges between 20 and 36 % across fuels and scenarios in 2025, converging toward 85-91 % by 2050 as FuelEU non-compliance penalties, growing proportionally to the widening gap between WtW GHG intensity and tightening annual targets, progressively overwhelm fuel expenditure. Its incidence is highest under S-low for all conventional pathways, confirming that low fossil prices amplify the relative weight of regulatory costs.

Based on the adopted projections, e-MeOH is the only fuel among those evaluated that remains competitive in the long term, despite its current cost being approximately six times higher than LNG. The expected price decrease over time, combined with its low-emission profile and the escalating FuelEU penalties on fossil alternatives, leads to an overall reduction in energy costs, making it the most advantageous pathway from 2040 onwards, provided the projected price floor is reached on schedule. The qualitative ranking of fuel pathways is therefore altered over the analysis horizon, with e-MeOH transitioning from the highest- to the lowest-cost option by 2040.

Arc elasticity statistics confirm near-unit price sensitivity for e-MeOH over 2025-2033, the only period during which scenario prices diverge. From 2034 onward, all scenarios converge to the floor price, rendering the elasticity undefined. Bio-MeOH shows the highest elasticity among all pathways, reflecting fuel-cost dominance with limited regulatory exposure. Conventional fuels display intermediate values (LNG: 0.360; HSFO: 0.436; MeOH: 0.521), decreasing over time as growing regulatory costs progressively dilute price sensitivity.

5.5.2 LNG methane slip

Regarding methane slip, the WtW GHG intensities of S_1, S_2 and S_3 are 91.0, 97.6, and 106.6 gCO_{2eq}/MJ, respectively, all exceeding the FuelEU 2025 threshold of 89.3 gCO_{2eq}/MJ. Consequently, the vessel incurs non-compliance penalties from the first reporting year under every methane slip scenario. In 2025, total energy costs range from €12.71 million (S_1) to €20.60 million (S_3), a differential of 62% driven entirely by the higher FuelEU penalty and ETS liability associated with greater slip. The corrected carbon intensity indicator CII^* equals 6.54, 7.13, and 7.94 for S_1- S_3, respectively, implying that the regulatory default systematically underestimates actual carbon intensity by up to 21 %. The arc elasticity E_{slip} decreases monotonically from approximately 0.68 in 2025 to 0.06 in 2050. This decline is not indicative of diminishing impact of methane slip but reflects a structural shift in cost composition: as FuelEU targets tighten, the absolute difference in penalties between scenarios remains approximately constant, since it is proportional to the fixed GHG WtW gap between S_1 and S_3, while the average energy costs grow substantially, compressing the relative metric. Accordingly, the regulatory share converges to approximately 90 % across all scenarios by 2045, a structural consequence of the 2050 FuelEU target lying a factor of 5-6 below the WtW intensity of any LNG pathway. This result indicates that, under the current FuelEU trajectory, continued LNG operation becomes financially untenable by approximately 2040-2045, regardless of methane slip mitigation, with penalties representing the dominant cost driver irrespective of engine technology. Tables and figures summarizing the results are reported in Appendix C.

5.6 Final remarks

The differences in emissions and energy costs among the three tested solutions are significant. International regulations on pollutant emissions are becoming increasingly stringent, and under the FuelEU initiative, the associated penalties can heavily impact total operational costs over the vessel's lifetime. Fossil-derived fuels (HSFO, LNG, and NG-MeOH) result in high emissions, while renewable-based fuels such as bio- and e-MeOH currently suffer from high production costs that hinder their immediate adoption. Consequently, lifetime energy costs increase either due to emissions-related penalties or the high price of the fuel itself.

Based on the adopted projections, e-MeOH is the only fuel among those evaluated that remains competitive in the long term, despite its current high price suggesting otherwise. The expected price decrease over time, combined with its low-emission profile, leads to an overall reduction in energy costs, making it particularly advantageous from 2040 onwards, when both HSFO and LNG become less economically viable. However, passenger ships collectively consume a very large amount of fuel: in 2024, the EU passenger and cruise sector accounted for 46.21 tonnes of total fuel consumption [128]. If MeOH were to become the main fuel for this segment, its lower calorific value would have significant implications. For the simulated route, the calculated consumption ratio between MeOH and conventional diesel configurations was 1.91, meaning that almost twice as much MeOH would be required to deliver the same energy. This lower energy density translates into both higher overall fuel volumes and reduced vessel autonomy, which in turn intensifies the need for adequate supply and storage infrastructure. Meeting such demand would require a fundamental transformation of fuel production and distribution systems. Large-scale deployment of e-MeOH would depend on the development of extensive renewable or nuclear-based hydrogen production, coupled with carbon capture, to ensure a sustainable supply chain. In parallel, a comprehensive network of coastal storage and bunkering facilities would need to be established, reaching a level of coverage at least comparable to today's HSFO or LNG infrastructure, to support regular cruise operations across European ports.

In addition to these logistical and production challenges, current e-MeOH prices remain significantly higher than those of conventional fuels. Achieving cost competitiveness will depend on economies of scale, which in turn rely on long-term investments and policy support. As a result, a rapid and complete transition to e-MeOH is not yet feasible under current market and infrastructure conditions. Nevertheless, given its strong long-term economic potential and alignment with EU decarbonization targets, building new passenger and cruise ships with methanol-ready configurations could offer both environmental benefits and a competitive advantage in the coming decades. For vessels expected to operate beyond 2040, such a strategy would facilitate future fuel switching and avoid costly retrofits, positioning operators favourably as e-MeOH production and bunkering networks expand. In the near future, within the considered operating context, a large cruise ship aiming to comply with international regulations shall significantly reduce its environmental footprint. Thus, the adoption of renewable fuels is mandatory across the entire supply chain, from production to combustion (WtW emissions). As demonstrated by the NG-MeOH test case, high upstream emissions from extraction, production, and transport can offset the benefits of low combustion emissions.

Moreover, the study highlights that the contribution of fossil fuels used in auxiliary systems, specifically in boilers and as pilot fuel for dual-fuel engines, while relatively small, is not negligible. In the bio- and e-MeOH scenarios, MGO accounts for the entirety of the TtW emissions, resulting in an excessive GHG intensity penalty by 2050 even in the bio-MeOH case for the analysed cruise. Replacing MGO with biodiesel or suitable blended alternatives could further reduce overall vessel emissions and help avoid such penalties. This approach could, in principle, also be extended to the direct replacement of HSFO with bio-based fuels. However, since renewable fuels currently remain more expensive than conventional options and their availability is still limited, the implementation of economic incentives and supportive policy measures will be essential to enable their broader adoption. On the other hand, their widespread use would face fewer infrastructural challenges, as existing fossil fuel storage and distribution facilities could largely be adapted for biofuel supply, reducing the need for entirely new bunkering networks.

The extension of the EU ETS to maritime transport carries combined significant economic consequences. The cost of carbon allowances has the potential to reshape freight rates, particularly on long-distance routes, while simultaneously encouraging both operational efficiency measures and investments in alternative fuels such as LNG, biofuels, and e-fuels. Yet, the regional scope of the measure creates concerns about competitive imbalances, as non-EU carriers may be disproportionately affected. To address this, part of the revenues from allowance auctions are directed toward the Innovation Fund and the Ocean Fund, designed to support research and the adoption of clean maritime technologies.

Despite its benefits, the EU ETS faces criticism regarding administrative burdens, exposure to volatile carbon markets, and the risk of carbon leakage through rerouted shipping services. Furthermore, questions remain about the effectiveness of a regional mechanism in addressing what is ultimately a global industry. Nevertheless, the EU's unilateral decision to include shipping within the EU ETS is widely recognised as a pivotal development in climate policy. It demonstrates both a commitment to reducing emissions within its jurisdiction and an effort to set an international precedent that could influence the establishment of broader, global market-based measures under the IMO.

FuelEU Maritime is expected to have an even higher transformative effect on the shipping sector by establishing a clear decarbonization pathway that stimulates demand for alternative fuels. This regulatory certainty encourages investment in production facilities, bunkering infrastructure, and vessel adaptations, helping to overcome the long-standing barriers to low-carbon fuel adoption. However, the regulation also raises concerns regarding fuel availability, competitiveness, and safety, particularly for emerging carriers such as hydrogen and ammonia, and may risk creating regional imbalances if not aligned with global supply chain developments. From a governance standpoint, FuelEU Maritime reflects the EU's strategy of combining market-based measures like the EU ETS with performance standards, thereby offering both economic incentives and technological guidance. This dual approach seeks to avoid the limitations of carbon pricing alone while preventing rigid technology mandates that could hinder flexibility. Its effectiveness will ultimately rely on robust enforcement, alignment with international frameworks such as the IMO's GHG strategy, and the shipping industry's ability to adapt to an evolving regulatory landscape. In fact, if global regulations are not established, there is a serious risk that older vessels will simply be relocated to operate outside EU waters, while newer vessels remain in the European market. Such a shift would undermine the effectiveness of regional measures, as it would not lead to the desired and necessary reduction in global CO_2 emissions from the whole maritime sector.

6. Conclusions

In this study, the 25-year energy costs of a large cruise ship operating in the Adriatic Sea are analysed, comparing the use of three different fuels: HSFO, LNG, and three types of MeOH. The calculations were conducted within the current regulatory framework (including EU and IMO regulations) for emission assessment, incorporating assumptions on fuel price evolution and carbon pricing over the considered time horizon.

The comparative analysis of emissions and energy costs across the evaluated fuel options reveals significant disparities. Fossil-derived fuels (HSFO, LNG, NG-MeOH) entail high emission profiles, while renewable alternatives such as bio- and e-MeOH remain constrained by the lower volumetric energy density, high production costs, limitations of production capacity and bunkering infrastructure. As international environmental regulations tighten under frameworks such as FuelEU and the EU ETS, lifetime operational costs are increasingly shaped either by emission-related penalties or by the premium price of low-carbon fuels. The fuel price sensitivity analysis confirms that e-MeOH in any case becomes the most economically competitive from 2040. Large-scale adoption in cruise shipping, however, would necessitate substantial renewable MeOH production capacity and expanded bunkering infrastructure. Methanol-ready vessels are already technically feasible. Therefore, new cruise ships intended to operate in Europe throughout their service life should be designed as methanol-ready from the outset. Nevertheless, under the current regulatory framework, the economic benefits would materialise only in the longer term; thus, public incentives remain necessary to accelerate the uptake of e-MeOH.

The methane slip sensitivity analysis shows that all LNG engine configurations examined exceed the FuelEU 2025 GHG threshold, generating non-compliance penalties from the first reporting year. The regulatory default value (3.1 %) systematically underestimates actual carbon intensity by up to 21 % compared to fleet-average operational measurements (6.4 %). By approximately 2040-2045, continued LNG operation will become financially untenable regardless of engine technology, as penalties converge to approximately 90 % of total energy costs. The study recommends revising emission accounting to reflect real operational methane slip values and confirms that LNG should be treated as a transitional rather than long-term solution. In any case, in the long term, the adoption of more realistic methane slip fractions gives a contribution to the total cost of energy, becoming negligible compared to the penalties due to the FuelEU Maritime Regulation. Therefore, only a swift correction of regulatory methane slip fractions can have a strong impact on the energy costs, inducing ship owners to switch toward more sustainable fuels.

The transition to renewable fuels underscores the importance of a full supply-chain (WtW) perspective: in particular, upstream emissions from fossil-derived MeOH can undermine the benefits of low combustion emissions, while partial reliance on MGO in dual-fuel systems further contributes to the carbon footprint. Substitution with biodiesel or blends could represent promising compliance pathways worthy of further investigation, as they could reduce overall energy costs while maintaining regulatory compliance both for conventional ships and for those already operating on alternative fuels. The inclusion of maritime transport in the EU ETS represents a turning point in climate governance, incentivising efficiency measures and low-carbon fuels but also raising concerns about competitive asymmetries, carbon leakage, and administrative burdens. FuelEU Maritime complements this approach by providing regulatory certainty and a decarbonization pathway that stimulates investment in alternative fuels, infrastructure, and vessel adaptation. Nevertheless, challenges remain regarding fuel availability, safety, and global alignment, particularly for emerging carriers such as hydrogen and ammonia.

The objective of the study is not to predict absolute fuel consumption with high pointwise accuracy, but to compare the relative impact of regulatory mechanisms and fuel choices under a consistent set of assumptions. However, this choice allows a consistent and transparent comparison of regulatory-driven operational costs across different fuels, independently of ship-specific investment strategies. Thus, several directions for future research are identified. First, since the simulation algorithm is applied deterministically, the results provide an overview of a specific case under average environmental conditions. The adoption of a probabilistic framework would enable a more robust, risk-based assessment of regulatory compliance, capturing and quantifying the uncertainties in environmental and operational conditions that a single deterministic scenario cannot represent. Second, the economic analysis could be strengthened through multi-scenario sensitivity analyses and extended to a full techno-economic assessment, including the capital expenditures associated with newbuilding and retrofit strategies for LNG- and MeOH-fuelled ships. Moreover, a full Life Cycle Assessment (LCA) of the evaluated fuel options represents a necessary next step, as it would broaden the scope of the analysis beyond operational energy costs and regulatory penalties, encompassing the wider environmental footprint of each fuel pathway. Third, in the CII calculations, the contribution of OPS is not included, although its use is planned under FuelEU. So, given that countries bordering the Adriatic Sea rely heavily on non-renewable electricity sources, a dedicated investigation should be conducted to assess the impact of OPS under different energy mix scenarios.

The findings of this study suggest that the window for a cost-effective transition to renewable marine fuels is approaching. Within an unbalanced and non-harmonised regulatory framework, the quantitative data produced by this study constitute a valuable reference for stakeholders operating under regulatory uncertainty. Moreover, the proposed methodology is directly transferable to other cruise vessel and operational scenarios, enabling similar assessments tailored to different contexts. Early investment in methanol-ready ship design, coupled with supportive policy mechanisms and infrastructure development, will be decisive in determining whether the cruise sector can align with the EU's long-term climate neutrality objectives.

NOMENCLATURE

CCS	Carbon Capture System	MARPOL	Marine Pollution
CII	Carbon Intensity Indicator	MeOH	Methanol
CH_4	Methane	MDO	Marine Diesel Oil
CO_2	Carbon Dioxide	MGO	Marine Gas Oil
DCS	Data Collect System	N_2O	Nitrous Oxide
DPF	Diesel Particulate Filters	NO_x	Nitrogen Oxides
ECA	Emission Control Area	OCCS	Onboard Carbon Capture System
EEDI	Energy Efficiency Design Index	OPS	Onshore Power Supply
EEXI	Energy Efficiency Existing Ship Index	PM	Particulate Matter
EF	Emission Coefficient	SCR	Selective Catalytic Reduction
EU ETS	European Union Emission Trading System	SECA	Sulphur Emission Control Area
EU	European Union	SEEMP	Ship Energy Efficiency Management Plan
FLL	Fuel Life Cycle Label	SPS	Sandwich Plate System
GFI	GHG Fuel Intensity	SO_x	Sulphur Oxides
GHG	Green House Gasses	RFNBO	Renewable Fuels of Non-Biological Origin
GT	Gross Tonnage	ULSFO	Ultra-Low Sulphur Fuel Oil
GWP	Global Warming Potential	UN	United Nations
HFO	Heavy Fuel Oil	VLSFO	Very-Low Sulphur Fuel Oil
HSFO	High Sulphur Fuel Oil	VOCs	Volatile Organic Compounds
IMO	International Maritime Organization	TtW	Tank-to-Wake
LCV	Lower Calorific Value	WtT	Well-to-Tank
LNG	Liquefied Natural Gas	WtW	Well-to-Wake

FUNDING

This study was carried out within the consortium iNEST (Interconnected North-Est Innovation Ecosystem) CUP J43C22000320006 funded by the European Union Next-GenerationEU (Piano Nazionale di Ripresa e Resilienza (PNRR)—Missione 4 Componente 2, Investimento 1.5—D.D. 1058 23/06/2022, ECS_00000043). This manuscript reflects only the Authors' views and opinions.

REFERENCES

[1] Mudryk, L. R., Dawson, J., Howell, S. E. L., Derksen, C., Zagon, T. A., Brady, M., 2021. Impact of 1, 2 and 4 °C of global warming on ship navigation in the Canadian Arctic. *Nature Climate Change*, 11(8), 673-679. https://doi.org/10.1038/s41558-021-01087-6

[2] EMSA, 2025. European Maritime Transport Environmental Report 2025. https://www.eea.europa.eu/en/analysis/publications/maritime-transport-2025 (accessed 8 September 2025)

[3] IMO, 2020. Fourth IMO GreenHouse Gas Study 2020

[4] EU, 2023. Regulation (EU) 2023/1805 On the use of renewable and low-carbon fuels in maritime transport, and amending Directive 2009/16/EC

[5] IMO, 2023. Resolution MEPC.377(80) 2023 IMO STRATEGY ON REDUCTION OF GHG EMISSIONS FROM SHIPS

[6] IMO, 2022. Resolution MEPC.364(79) 2022 GUIDELINES ON THE METHOD OF CALCULATION OF THE ATTAINED ENERGY EFFICIENCY DESIGN INDEX (EEDI) FOR NEW SHIPS

[7] IMO, 2022. Resolution MEPC.365(79) 2022 GUIDELINES ON SURVEY AND CERTIFICATION OF THE ENERGY EFFICIENCY DESIGN INDEX (EEDI)

[8] IMO, 2022. Resolution MEPC.350(78) 2022 GUIDELINES ON THE METHOD OF CALCULATION OF THE ATTAINED ENERGY EFFICIENCY EXISTING SHIP INDEX (EEXI)

[9] IMO, 2022. Resolution MEPC.351(78) 2022 GUIDELINES ON SURVEY AND CERTIFICATION OF THE ATTAINED ENERGY EFFICIENCY EXISTING SHIP INDEX (EEXI)

[10] IMO, 2022. Resolution MEPC.352(78) 2022 GUIDELINES ON OPERATIONAL CARBON INTENSITY INDICATORS AND THE CALCULATION METHODS (CII GUIDELINES, G1)

[11] IMO, 2022. Resolution MEPC.353(78) 2022 GUIDELINES ON THE REFERENCE LINES FOR USE WITH OPERATIONAL CARBON INTENSITY INDICATORS (CII REFERENCE LINES GUIDELINES, G2)

[12] IMO, 2022. Resolution MEPC.354(78) 2022 GUIDELINES ON THE OPERATIONAL CARBON INTENSITY RATING OF SHIPS (CII RATING GUIDELINES, G4)

[13] IMO, 2022. Resolution MEPC.355(78) 2022 INTERIM GUIDELINES ON CORRECTION FACTORS AND VOYAGE ADJUSTMENTS FOR CII CALCULATIONS (CII GUIDELINES, G5)

[14] EU, 2023. Regulation (EU) 2023/957 of the European Parliament and of the Council amending Regulation (EU) 2015/757 in order to provide for the inclusion of maritime transport activities in the EU Emissions Trading System and for the monitoring, reporting and verification of emissions of additional greenhouse gases and emissions from additional ship types

[15] EU, 2023. Directive (EU) 2023/959 Amending Directive 2003/87/EC establishing a system for greenhouse gas emission allowance trading within the Union and Decision (EU) 2015/1814 concerning the establishment and operation of a market stability reserve for the Union greenhouse gas emission trading system

[16] EU, 2015. Regulation (EU) 2015/757 On the monitoring, reporting and verification of carbon dioxide emissions from maritime transport, and amending Directive 2009/16/EC

[17] IMO, 2025. MEPC 83/17 - REPORT OF THE MARINE ENVIRONMENT PROTECTION COMMITTEE ON ITS EIGHTY-THIRD SESSION

[18] Li, Y., Wang, Z., Li, M., Ji, Y., Han, F., 2026. Energy Efficiency Analysis and Design Research of Hydrogen Fuel Cell Powered Ships. *Proceedings of the 1st Conference on Transportation and Energy Integration Technologies* (C-TEIT 2025), 25-27 July, Dalian, China, 55-62. https://doi.org/10.1007/978-981-95-6754-6_6

[19] Hoang, A. T., Pandey, A., Martinez De Osés, F. J., Chen, W.-H., Said, Z., Ng, K. H., Ağbulut, Ü., Tarełko, W., Ölçer, A. I., Nguyen, X. P., 2023. Technological solutions for boosting hydrogen role in decarbonization strategies and net-zero goals of world shipping: Challenges and perspectives. *Renewable and Sustainable Energy Reviews*, 188, 113790. https://doi.org/10.1016/j.rser.2023.113790

[20] Utzeri, S., Braidotti, L., Bertagna, S., Padolecchia, D., Taucer Marchesi, N., Del Piero, E., Bucci, V., Marino', A., 2025. Optimisation of a Hybrid-Parallel Power Train for a Aframax Tanker to Minimise Emissions in Every Operative Condition. In *Technology and Science for the Ships of the Future*, IOS Press, 980-989. https://doi.org/10.3233/PMST250116

[21] Mao, R., Qian, Y., Liu, K., Li, Y., Li, G., Zhang, H., 2025. A comprehensive survey of battery energy in maritime transportation: Trends, challenges, and future perspectives. *Ocean Engineering*, 337, 121881. https://doi.org/10.1016/j.oceaneng.2025.121881

[22] Lafoz, M., Navarro, G., Blanco, M., Nájera, J., Rausell, E., Munilla, J., 2025. Analysis of energy storage solutions for ship maneuvering in ports. *Power Electronic Devices and Components*, 12, 100109. https://doi.org/10.1016/j.pedc.2025.100109

[23] Diaz, R., Smith, K., Bertagna, S., Bucci, V., 2022. Digital Transformation, Applications, and Vulnerabilities in Maritime and Shipbuilding Ecosystems. *Procedia Computer Science*, 217, 1396-1405. https://doi.org/10.1016/j.procs.2022.12.338

[24] Padolecchia, D., Bertagna, S., Braidotti, L., Bucci, V., Marino', A., 2025. Evaluating Virtual Prototyping Approaches in Integrated Ship Design: A Case-Based Analysis. *International Journal on Interactive Design and Manufacturing (IJIDeM)*. https://doi.org/10.1007/s12008-025-02370-y

[25] Bortuzzo, V., Bertagna, S., Bucci, V., 2023. Mitigation of CO2 Emissions from Commercial Ships: Evaluation of the Technology Readiness Level of Carbon Capture Systems. *Energies*, 16(9), 3646. https://doi.org/10.3390/en16093646

[26] Mallouppas, G., Yfantis, E. Ar., 2021. Decarbonization in Shipping industry: A review of research, technology development, and innovation proposals. *Journal of Marine Science and Engineering*, 9(4), 415. https://doi.org/10.3390/jmse9040415

[27] Zincir, B., 2023. Slow steaming application for short-sea shipping to comply with the CII regulation. *Brodogradnja*, 74(2), 21-38. https://doi.org/10.21278/brod74202

[28] Bortuzzo, V., Bertagna, S., Braidotti, L., Bucci, V., 2025. An innovative tool for the evaluation of energy efficiency of merchant ships. *Brodogradnja*, 76(3), 76304. https://doi.org/10.21278/brod76304

[29] Hoang, A. T., Bui, T. A. E., Nguyen, X. P., Bui, V. H., Nguyen, Q. C., Truong, T. H., Chung, N., 2025. Explainable machine learning-based prediction of fuel consumption in ship main engines using operational data. *Brodogradnja*, 76(4), 76405. https://doi.org/10.21278/brod76405

[30] Fan, A., Yang, J., Yang, L., Wu, D., Vladimir, N., 2022. A review of ship fuel consumption models. *Ocean Engineering*, 264, 112405. https://doi.org/10.1016/j.oceaneng.2022.112405

[31] Sontakke, I., Bergström, M., Gosala, V., Baldauf, M., Ehlers, S., 2026. Techno-economic analysis of decarbonization pathways for a deep-sea container vessel. *Ship Technology Research*, 73(1), 41-58. https://doi.org/10.1080/09377255.2025.2585247

[32] Zheng, Q., Sun, L., Chang, S., Xing, H., 2025. Techno-Economic Analysis of Multi-Purpose Heavy-Lift Vessels Using Methanol as Fuel. *Journal of Marine Science and Engineering*, 13(7), 1234. https://doi.org/10.3390/jmse13071234

[33] Flodén, J., Zetterberg, L., Christodoulou, A., Parsmo, R., Fridell, E., Hansson, J., Rootzén, J., Woxenius, J., 2024. Shipping in the EU emissions trading system: implications for mitigation, costs and modal split. *Climate Policy*, 24(7), 969-987. https://doi.org/10.1080/14693062.2024.2309167

[34] Esteve-Pérez, J., Río-González, M. del, Gutiérrez-Romero, J. E., 2023. Forecast Analysis of Pollutant Emissions of Cruise Ship Routes in Western Mediterranean. *Applied Sciences*, 13(14), 8149. https://doi.org/10.3390/app13148149

[35] Braidotti, L., Utzeri, S., Del Piero, E., Marino', A., 2025. Impact of New Environmental Rules on the Fuel and Emissions Costs of a Mediterranean Cruise. In *Technology and Science for the Ships of the Future*, IOS Press, 156-165. https://doi.org/10.3233/PMST250021

[36] Zamboni, G., Scamardella, F., Gualeni, P., Canepa, E., 2024. Comparative analysis among different alternative fuels for ship propulsion in a well-to-wake perspective. *Heliyon*, 10(4), e26016. https://doi.org/10.1016/j.heliyon.2024.e26016

[37] Acanfora, M., Altosole, M., Balsamo, F., Mocerino, L., Scamardella, F., Campora, U., 2025. A Technical, Environmental and Economical Comparison Among Traditional and Unconventional Marine Fuels. *TransNav, International Journal on Marine Navigation and Safety od Sea Transportation*, 19(3), 725-734. https://doi.org/10.12716/1001.19.03.04

[38] Dragović, B., Tzannatos, E., Tselentis, V., Meštrović, R., Škurić, M., 2018. Ship emissions and their externalities in cruise ports. *Transportation Research Part D: Transport and Environment*, 61, 289-300. https://doi.org/10.1016/j.trd.2015.11.007

[39] Kerbiriou, R., Serry, A., Alix, Y., 2025. Estimating pollutant emissions from sea cruise in the Adriatic Sea in 2022 and regulatory measures. Transportation Research Procedia, 83, 149-156. https://doi.org/10.1016/j.trpro.2025.02.021

[40] Balcombe, P., Staffell, I., Kerdan, I. G., Speirs, J. F., Brandon, N. P., Hawkes, A. D., 2021. How can LNG-fuelled ships meet decarbonisation targets? An environmental and economic analysis. *Energy*, 227, 120462. https://doi.org/10.1016/j.energy.2021.120462

[41] Hoang, A. T., Chen, W.-H., López-Escalante, M. C., Guerrero-Pérez, M. O., Rodríguez-Castellón, E., Kowalski, J., Le, T. T., Bui, V. G., Nguyen, X. P., 2026. Methanol for decarbonization of the maritime sector: From ideological strategy to practical solutions. *Renewable and Sustainable Energy Reviews*, 229, 116638. https://doi.org/10.1016/j.rser.2025.116638

[42] Zhang, Y., Chen, P., Wu, D., Hao, X., Yang, T., Cairns, A., 2025. Advancing maritime decarbonisation: Design and optimisation of ammonia-fuelled propulsion systems. *Journal of Cleaner Production*, 535, 147145. https://doi.org/10.1016/j.jclepro.2025.147145

[43] EMSA, 2024. Safety of Ammonia for Use in Ships. https://emsa.europa.eu/publications/download/7881/5264/23.html

[44] Alavi-Borazjani, S. A., Adeel, S., Chkoniya, V., 2025. Hydrogen as a Sustainable Fuel: Transforming Maritime Logistics. *Energies*, 18(5), 1231. https://doi.org/10.3390/en18051231

[45] Bertagna, S., Kouznetsov, I., Braidotti, L., Marinò, A., Bucci, V., 2023. A Rational Approach to the Ecological Transition in the Cruise Market: Technologies and Design Compromises for the Fuel Switch. *Journal of Marine Science and Engineering*, 11(1), 67. https://doi.org/10.3390/jmse11010067

[46] Braidotti, L., Utzeri, S., Bertagna, S., Bucci, V., 2024. A fast simulation method for the probabilistic assessment of emissions in cruise ship's itinerary planning. *Ocean Engineering*, 311, 118804. https://doi.org/10.1016/j.oceaneng.2024.118804

[47] IMO, 2024. Resolution MEPC.391(81) 2024 GUIDELINES ON LIFE CYCLE GHG INTENSITY OF MARINE FUELS (2024 LCA GUIDELINES)

[48] IMO, 2023. MEPC 83/6 ENERGY EFFICIENCY OF SHIPS Report on annual carbon intensity and efficiency of the fleet (Reporting year: 2023) Note by the Secretariat

[49] IMO, 2024. Resolution MEPC.395(82) 2024 GUIDELINES FOR THE DEVELOPMENT OF A SHIP ENERGY EFFICIENCY MANAGEMENT PLAN (SEEMP)

[50] Lloyd Register, 2025. IMO Marine Environment Protection Committee (MEPC 83) - Summary Report

[51] Díaz-Cuenca, D., Villalba-Herreros, A., Leo, T. J., d'Amore-Domenech, R., 2025. Alternative Fuels in the Maritime Industry: Emissions Evaluation of Bulk Carrier Ships. *Journal of Marine Science and Engineering*, 13(7), 1313. https://doi.org/10.3390/jmse13071313

[52] Yuksel, O., Goksu, B., 2025. Effects of transportation of electric vehicles by a RoPax ship on carbon intensity and energy efficiency. *Sustainable Energy Technologies and Assessments*, 75, 104238. https://doi.org/10.1016/j.seta.2025.104238

[53] Lam, J. S. L., Piga, B., Zengqi, X., 2022. Role of bio-LNG in shipping industry decarbonisation. Maritime Energy and Sustainable Development Centre of Excellence (MESD CoE), Nanyang Technological University, Singapore

[54] Yuan, Q., Wang, S., Peng, J., 2023. Operational efficiency optimization method for ship fleet to comply with the carbon intensity indicator (CII) regulation. *Ocean Engineering*, 286, 115487. https://doi.org/10.1016/j.oceaneng.2023.115487

[55] Zhang, Y., Xiao, Y., Teng, F., Li, T., 2025. Distributed optimal energy management strategy for S-IES with IMO's regulation on CII. *Ocean Engineering*, 340, 122397. https://doi.org/10.1016/j.oceaneng.2025.122397

[56] Braidotti, L., Bertagna, S., Rappoccio, R., Utzeri, S., Bucci, V., Marinò, A., 2023. On the inconsistency and revision of Carbon Intensity Indicator for cruise ships. *Transportation Research Part D: Transport and Environment*, 118, 103662. https://doi.org/10.1016/j.trd.2023.103662

[57] IMO, 2023. Regulation MEPC.376(80) GUIDELINES ON LIFE CYCLE GHG INTENSITY OF MARINE FUELS (LCA GUIDELINES)

[58] UN, 2021. Global Roadmap for Accelerated SDG7 Action in Support of the 2030 Agenda for Sustainable Development and the Paris Agreement on Climate Change

[59] EU, 2024. Fit for 55 package - BRIEFING Towards climate neutrality

[60] Deng, S., Mi, Z., 2023. A review on carbon emissions of global shipping. *Marine Development*, 1(1), 4. https://doi.org/10.1007/s44312-023-00001-2

[61] Lun, Y. H. V., Lai, K., Cheng, T. C. E., Yang, D., 2023. International Trade and Shipping. In *Shipping and Logistics Management*, Springer International Publishing, Cham, 3-20. https://doi.org/10.1007/978-3-031-26090-2_1

[62] Christodoulou, A., Gonzalez-Aregall, M., Linde, T., Vierth, I., Cullinane, K., 2019. Targeting the reduction of shipping emissions to air: A global review and taxonomy of policies, incentives and measures. *Maritime Business Review*, 4(1), 16-30. https://doi.org/10.1108/MABR-08-2018-0030

[63] EU, 2024. The EU ETS and MRV Maritime General guidance for shipping companies

[64] EU, 2018. Directive (EU) 2018/2001 On the promotion of the use of energy from renewable sources (recast)

[65] Zamiatina, N., 2016. Comparative Overview of Marine Fuel Quality on Diesel Engine Operation. *Procedia Engineering*, 134, 157-164. https://doi.org/10.1016/j.proeng.2016.01.055

[66] IMO, 2025. International Convention for the Prevention of Pollution from Ships (MARPOL) Annex VI - Regulations for the Prevention of Air Pollution from Ships (Resolution MEPC.385(81))

[67] Bilousov, I., Bulgakov, M., Savchuk, V., 2020. *Modern Marine Internal Combustion Engines: A Technical and Historical Overview*, Springer International Publishing, Cham. https://doi.org/10.1007/978-3-030-49749-1

[68] Bukovac, O., Pelić, V., Mrakovčić, T., Jelić, M., Radica, G., Vidović, T., et al., 2025. Remote Monitoring, Simulation and Diagnosis of Electronically Controlled Marine Engines. *Energies*, 18(6), 1399. https://doi.org/10.3390/en18061399

[69] Shahid, S. M., Ko, S., Kwon, S., 2019. Real-Time Classification of Diesel Marine Engine Loads Using Machine Learning. *Sensors*, 19(14), 3172. https://doi.org/10.3390/s19143172

[70] Zhu, S., Zhang, K., Deng, K., 2020. A review of waste heat recovery from the marine engine with highly efficient bottoming power cycles. *Renewable and Sustainable Energy Reviews*, 120, 109611. https://doi.org/10.1016/j.rser.2019.109611

[71] Radica, G., Vidović, T., Šimunović, J., Jurić, Z., 2025. Overview of Hybrid Marine Energy System Configurations and System Component Modeling Approaches. *Energies*, 18(5), 1189. https://doi.org/10.3390/en18051189

[72] Mahía Prados, J. M., Arias Fernández, I., Romero Gómez, M., Parga, M. N., 2024. The decarbonisation of the maritime sector: Horizon 2050. *Brodogradnja*, 75(2), 75202. https://doi.org/10.21278/brod75202

[73] Napolitano, P., Liotta, L. F., Guido, C., Tornatore, C., Pantaleo, G., La Parola, V., Beatrice, C., 2022. Insights of Selective Catalytic Reduction Technology for Nitrogen Oxides Control in Marine Engine Applications. *Catalysts*, 12(10), 1191. https://doi.org/10.3390/catal12101191

[74] Choi, W., Choi, S., Na, S., Shin, D., Jeong, H., Sung, Y., 2024. Numerical Study on Compact Design in Marine Urea-SCR Systems for Small Ship Applications. *Energies*, 17(1), 187. https://doi.org/10.3390/en17010187

[75] Lehtoranta, K., Aakko-Saksa, P., Murtonen, T., Vesala, H., Ntziachristos, L., Rönkkö, T., Karjalainen, P., Kuittinen, N., Timonen, H., 2019. Particulate Mass and Nonvolatile Particle Number Emissions from Marine Engines Using Low-Sulfur Fuels, Natural Gas, or Scrubbers. *Environmental Science & Technology*, 53(6), 3315-3322. https://doi.org/10.1021/acs.est.8b05555

[76] Ma, R., Zhao, Q., Wang, K., Cao, J., Yang, C., Hu, Z., Huang, L., 2025. Energy efficiency improvement technologies for ship in operation: A comprehensive review. *Ocean Engineering*, 331, 121258. https://doi.org/10.1016/j.oceaneng.2025.121258

[77] SRC, 2023. Press Relase - Approval in Principle for Methanol Superstorage solution on existing ships. https://nova.src.ee/storage/media/483/SRC_secures_AiP.pdf

[78] Lloyd Register, 2025. LR-RU-012 Rules and Regulations for the Classification of Ships using Gases or other Low-flashpoint Fuels

[79] Methanol Institute, 2016. Methanol Technical Data Sheet. https://methanolorg.wpenginepowered.com/wp-content/uploads/2016/06/Methanol-Technical-Data-Sheet.pdf

[80] Pereira, E. G., 2025. The implications and challenges of the IMO 2020 regulation: Exploring options for compliance. *Review of European, Comparative & International Environmental Law*, 34(1), 246-261. https://doi.org/10.1111/reel.12593

[81] Prause, G., Olaniyi, E. O., 2019. A compliance cost analysis of the SECA regulation in the Baltic Sea. *Entrepreneurship and Sustainability Issues*, 6(4), 1907-1921. https://doi.org/10.9770/jesi.2019.6.4(26)

[82] Herdzik, J., 2011. LNG as a marine fuel - possibilities and problem. *Journal of KONES*, 18(2), 169-176.

[83] Chorowski, M., Duda, P., Polinski, J., Skrzypacz, J., 2015. LNG systems for natural gas propelled ships. *IOP Conference Series: Materials Science and Engineering*, 101, 012089. https://doi.org/10.1088/1757-899X/101/1/012089

[84] Sambucci, M., Savoni, F., Valente, M., 2023. Aerogel Technology for Thermal Insulation of Cryogenic Tanks—Numerical Analysis for Comparison with Traditional Insulating Materials. *Gels*, 9(4), 307. https://doi.org/10.3390/gels9040307

[85] IMO, 2015. Resolution MSC.391(95) 2015 ADOPTION OF THE INTERNATIONAL CODE OF SAFETY FOR SHIPS USING GASES OR OTHER LOW-FLASHPOINT FUELS (IGF CODE)

[86] Nsaif, O., Kokjohn, S., Hessel, R., Dempsey, A., 2024. Reducing Methane Emissions From Lean Burn Natural Gas Engines With Prechamber Ignited Mixing-Controlled Combustion. *Journal of Engineering for Gas Turbines and Power*, 146(6), 061023. https://doi.org/10.1115/1.4064454

[87] Tay, Z. Y., Konovessis, D., 2023. Sustainable energy propulsion system for sea transport to achieve United Nations sustainable development goals: a review. *Discover Sustainability*, 4(1), 20. https://doi.org/10.1007/s43621-023-00132-y

[88] Zhang, W., Wang, J., Qin, G., Kuntal, S., Gong, F., Yan, R., 2025. Review of the state-of-the-art of alternative marine fuels: A viable approach to zero-carbon shipping. *Cleaner Logistics and Supply Chain*, 16, 100232. https://doi.org/10.1016/j.clscn.2025.100232

[89] Peng, Y., Zhao, X., Zuo, T., Wang, W., Song, X., 2021. A systematic literature review on port LNG bunkering station. *Transportation Research Part D: Transport and Environment*, 91. https://doi.org/10.1016/j.trd.2021.102704

[90] Agyekum, E. B., Okonkwo, P. C., Rashid, F. L., 2025. Research on biomass energy and CO2 conversion to methanol: a combination of conventional and bibliometric review analysis. *Carbon Research*, 4(1), 4. https://doi.org/10.1007/s44246-024-00179-0

[91] Deka, T. J., Osman, A. I., Baruah, D. C., Rooney, D. W., 2022. Methanol fuel production, utilization, and techno-economy: a review. *Environmental Chemistry Letters*, 20(6), 3525-3554. https://doi.org/10.1007/s10311-022-01485-y

[92] Ullah, A., Hashim, N. A., Rabuni, M. F., Mohd Junaidi, M. U., 2023. A Review on Methanol as a Clean Energy Carrier: Roles of Zeolite in Improving Production Efficiency. *Energies*, 16(3), 1482. https://doi.org/10.3390/en16031482

[93] Wu, P.-C., Lin, C.-Y., 2025. Feasibility and Cost-Benefit Analysis of Methanol as a Sustainable Alternative Fuel for Ships. *Journal of Marine Science and Engineering*, 13(5), 973. https://doi.org/10.3390/jmse13050973

[94] IMO, 2016. Methanol as Marine Fuel: Environmental Benefits, Technology Readiness, and Economic Feasibility

[95] Guo, H., Başhan, V., Yu, C., Bolat, F., Demirel, H., Tian, X., 2025. Effect of Methanol Injection Timing on Performance of Marine Diesel Engines and Emission Reduction. *Journal of Marine Science and Engineering*, 13(5), 949. https://doi.org/10.3390/jmse13050949

[96] Parris, D., Spinthiropoulos, K., Ragazou, K., Giovou, A., Tsanaktsidis, C., 2024. Methanol, a Plugin Marine Fuel for Green House Gas Reduction—A Review. *Energies*, 17(3), 605. https://doi.org/10.3390/en17030605

[97] Fossen, T. I., 2011. *Handbook of Marine Craft Hydrodynamics and Motion Control*

[98] Blendermann, W., 2014. Book review: Practical Ship and Offshore Structure Aerodynamics. *Ship Technology Research*, 61(2), 110-111. https://doi.org/10.1179/str.2014.61.2.004

[99] Liu, S., Papanikolaou, A., 2020. Regression analysis of experimental data for added resistance in waves of arbitrary heading and development of a semi-empirical formula. *Ocean Engineering*, 206, 107357. https://doi.org/10.1016/j.oceaneng.2020.107357

[100] Molland, A. F., Turnock, S. R., 2011. *Marine Rudders and Control Surfaces: Principles, Data, Design and Applications*. Elsevier

[101] Coleman, T. F., Li, Y., 1994. On the convergence of interior-reflective Newton methods for nonlinear minimization subject to bounds. *Mathematical Programming*, 67(1), 189-224. https://doi.org/10.1007/BF01582221

[102] Coleman, T. F., Li, Y., 1996. An interior trust region approach for nonlinear minimization subject to bounds. *SIAM Journal on Optimization*, 6(2), 418-445. https://doi.org/10.1137/0806023

[103] Moré, J. J., Garbow, B. S., Hillstrom, K. E., 1980. User guide for MINPACK-1. CM-P00068642. https://cds.cern.ch/record/126569/files/CM-P00068642 (accessed 3 May 2025)

[104] Powell, M. J. D., 1968. A Fortran subroutine for Solving Systems of Nonlinear Algebraic Equations. Technical Report AERE-R 5947, Atomic Energy Research Establishment, Harwell, Berkshire, UK. https://scholar.google.com/scholar_lookup?title=A%20Fortran%20Subroutine%20for%20Solving%20Systems%20of%20Nonlinear%20Algebraic%20Equations%3A%20Technical%20Report&publication_year=1968&author=M.J.%20Powell (accessed 3 May 2025)

[105] NGIA, 2025. World Port Index - National Geospatial-Intelligience Agency. https://msi.nga.mil/Publications/APC (accessed 1 March 2025)

[106] Katalinić, M., Parunov, J., 2021. Comprehensive wind and wave statistics and extreme values for design and analysis of marine structures in the adriatic sea. *Journal of Marine Science and Engineering*, 9(5), 522. https://doi.org/10.3390/jmse9050522

[107] Moskowitz, L. I., Pierson, W. J., Mehr, E., 1962. Wave spectra estimated from wave records obtained by the OWS weather explorer and the OWS weather reporter. https://doi.org/10.21236/AD0293451

[108] Faltinsen, O. M., 1980. Prediction of resistance and propulsion of a ship in a seaway. 1980, 505-529.

[109] Lang, X., Mao, W., 2020. A semi-empirical model for ship speed loss prediction at head sea and its validation by full-scale measurements. *Ocean Engineering*, 209, 107494. https://doi.org/10.1016/j.oceaneng.2020.107494

[110] Kresic, 1983. Effects of propeller design-point definition on the performance of a propeller. https://scholar.google.com/scholar_lookup?title=Effects%20of%20propeller%20designpoint%20definition%20on%20the%20performance%20of%20a%20propeller&publication_year=1983&author=M.%20Kresic&author=B.%20Haskell (accessed 3 May 2025)

[111] Holtrop, J., Mennen, G. G. J., 1982. An approximate power prediction method. *International Shipbuilding Progress*, 29(335), 166-170. https://doi.org/10.3233/ISP-1982-2933501

[112] Lackemby, H., 1964. The Effect of Shallow Water on Ship Speed. *Naval Engineers Journal*, 76(1), 21-26. https://doi.org/10.1111/j.1559-3584.1964.tb04413.x

[113] EU, 2023. Directive (EU) 2023/2413 amending Directive (EU) 2018/2001, Regulation (EU) 2018/1999 and Directive 98/70/EC as regards the promotion of energy from renewable sources, and repealing Council Directive (EU) 2015/652

[114] EU, 2023. Commission Delegated Regulation (EU) 2023/2776 mending Regulation (EU) 2015/757 of the European Parliament and of the Council as regards the rules for monitoring greenhouse gas emissions and other relevant information from maritime transport

[115] EU, 2020. Corrigenda (EU) Corrigendum to Directive (EU) 2018/2001 of the European Parliament and of the Council of 11 December 2018 on the promotion of the use of energy from renewable sources

[116] Methanol Institute, 2022. Carbon Footprint of Methanol

[117] IMO, 2021. Resolution MEPC.338(76) 2021 GUIDELINES ON THE OPERATIONAL CARBON INTENSITY REDEUCTION FACTORS RELATIVE TO REFERENCE LINES (CII REDUCTION FACTORS GUIDELINES, G3)

[118] ECB, 2025. Economic Bulletin

[119] 2025. Global Average Bunker Prices. https://shipandbunker.com/prices/av/global/av-glb-global-average-bunker-price (accessed 6 May 2025)

[120] Jeroen Dierickx, 2024. Economic Value of methanol for shipping under FuelEU maritime and EU-ETS

[121] Methanex, 2025. Methanex Monthly Average Regional Posted Contract Price History. https://www.methanex.com/wp-content/uploads/MxAvgPrice-April-29-2025.xls (accessed 25 April 2025)

[122] Trading Economics, 2025. UE Natural gas Pricing. https://it.tradingeconomics.com/commodity/eu-natural-gas (accessed 7 May 2025)

[123] Leisner, M., Eide, M. S., Sekkesæter, Ø., Endresen, Ø., Hammer, L., Mjelde, A., 2025. Methanol Fuel in Shipping. DNV.

[124] Kuittinen, N., Koponen, P., Vesala, H., Lehtoranta, K., 2024. Methane slip and other emissions from newbuild LNG engine under real-world operation of a state-of-the art cruise ship. *Atmospheric Environment: X*, 23, 100285. https://doi.org/10.1016/j.aeaoa.2024.100285

[125] Comer, B., Beecken, J., Vermeulen, R., Sturrup, E., Paschinger, P., Osipova, L., et al., 2024. Fugitive And Unburned Methane Emissions from Ships (FUMES).

[126] ISO, 2015. ISO Ships and marine technology — Guidelines for the assessment of speed and power performance by analysis of speed trial data. https://www.iso.org/standard/61902.html (accessed 8 September 2025)

[127] Wärtsilä, 2024. Engines and Generating Sets. https://www.wartsila.com/marine/products/engines-and-generating-sets

[128] EU, 2025. THETIS-MRV – Supporting Monitoring, Reporting and Verification of CO2 Emissions from Maritime Transport. European Maritime Safety Agency. https://mrv.emsa.europa.eu/#public/emission-report (accessed 26 September 2025)

APPENDIX A

Table A1 presents the detailed schedule of the original itinerary. For each subleg, the operational phase, the length, the duration, the start time, and the velocity are reported.

Table A1 Detailed Schedule and discretization of original itinerary

nSubLeg	Type	Leg	Length [mn]	Δt [h]	Start time [hh:mm]	Vt [kn]
1	Port Stay	ITVCE	0.0	0.1	16:00	0.0
2	Maneuvering	ITVCE	0.1	0.1	16:05	1.0
3	Transit	ITVCE → SIKOP	0.3	0.2	16:09	3.0
4	Navigation	ITVCE → SIKOP	4.4	0,7	16:18	7.4
5	Navigation	ITVCE → SIKOP	2.1	0.1	16:59	9.7
6	Navigation	ITVCE → SIKOP	5.3	0.7	17:03	10.3
7	Navigation	ITVCE → SIKOP	30.6	3.8	17:47	8.4
8	Navigation	ITVCE → SIKOP	13.8	1.5	21:35	9.3
9	Navigation	ITVCE → SIKOP	24.5	3.4	23:07	7.7
10	Navigation	ITVCE → SIKOP	34.5	3.0	02:33	9.7
11	Navigation	ITVCE → SIKOP	2.5	0.5	05:32	6.2
12	Navigation	ITVCE → SIKOP	0.5	0.1	06:03	1.8
13	Transit	ITVCE → SIKOP	0.3	0.2	06:09	2.9
14	Maneuvering	SIKOP	0.2	0.2	06:18	1.9
15	Port Stay	SIKOP	0.0	9.2	06:27	0.0
16	Maneuvering	SIKOP	0.3	0.1	15:38	1.3
17	Transit	SIKOP → HRZAD	0.1	0.0	15:42	4.2
18	Navigation	SIKOP → HRZAD	1.8	0.2	15:44	7.3
19	Navigation	SIKOP → HRZAD	0.9	0.2	15:58	10.6
20	Navigation	SIKOP → HRZAD	10.9	1.5	16:08	12.7
21	Navigation	SIKOP → HRZAD	26.9	2.1	17:35	13.1
22	Navigation	SIKOP → HRZAD	11.8	3.0	19:43	12.7
23	Navigation	SIKOP → HRZAD	45.5	1.3	22:43	10.9
24	Navigation	SIKOP → HRZAD	3.3	0.4	23:58	9.1

25	Navigation	SIKOP → HRZAD	7.9	0.6	00:22	11.6
26	Navigation	SIKOP → HRZAD	1.3	0.4	00:59	11.9
27	Navigation	SIKOP → HRZAD	6.3	0.4	01:21	10.1
28	Navigation	SIKOP → HRZAD	51.4	4.1	01:47	12.5
29	Navigation	SIKOP → HRZAD	3.7	0.3	05:51	11.5
30	Navigation	SIKOP → HRZAD	1.5	0.1	06:06	8.5
31	Navigation	SIKOP → HRZAD	0.4	0.1	06:11	5.5
32	Transit	SIKOP → HRZAD	0.4	0.2	06:16	3.3
33	Maneuvering	HRZAD	0.1	0.5	06:25	1.3
34	Port Stay	HRZAD	0.0	8.7	06:57	0.0
35	Maneuvering	HRZAD	0.2	0.2	15:37	1.1
36	Transit	HRZAD → ITVCE	0.6	0.1	15:50	4.3
37	Navigation	HRZAD → ITVCE	0.8	0.1	15:55	8.6
38	Navigation	HRZAD → ITVCE	3.5	0.5	16:02	11.4
39	Navigation	HRZAD → ITVCE	45.4	4.6	16:32	12.9
40	Navigation	HRZAD → ITVCE	30.7	1.7	21:08	11.3
41	Navigation	HRZAD → ITVCE	17.9	2.4	22:48	9.9
42	Navigation	HRZAD → ITVCE	44.4	3.3	01:10	11.4
43	Navigation	HRZAD → ITVCE	9.4	0.5	04:29	12.1
44	Navigation	HRZAD → ITVCE	4.0	0.4	05:00	11.0
45	Navigation	HRZAD → ITVCE	2.9	0.4	05:22	9.4
46	Navigation	HRZAD → ITVCE	2.8	0.3	05:45	7.2
47	Transit	HRZAD → ITVCE	0.1	0.0	06:05	1.7
48	Maneuvering	ITVCE	0.2	0.2	06:07	1.6
49	Port Stay	ITVCE	0.0	9.7	06:16	0.0

APPENDIX B

FuelEU penalty and EU ETS totals evolution in 2025-2050 for each fuel considered are reported in Figures B1 and B2.

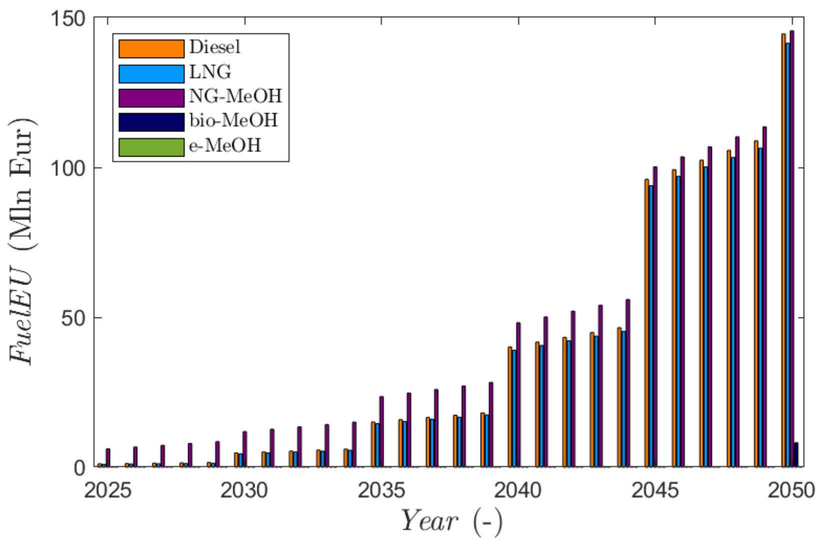

Fig. B1 FuelEU penalty 2025-2050 – All fuels

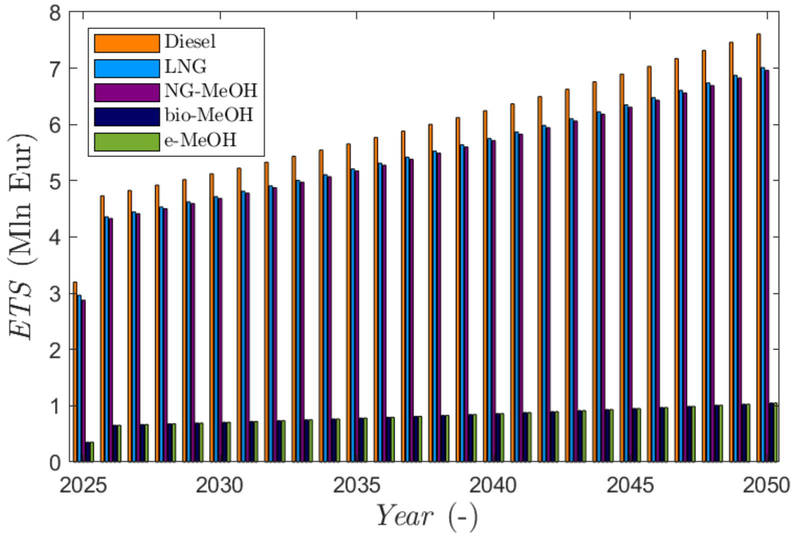

Fig. B2 EU ETS in 2025-2050 – All fuels

APPENDIX C

This appendix collects the graphical and tabular outputs of the two sensitivity analyses described in Section 3.6 and discussed in Section 5.5. For the fuel price sensitivity, Figures C.1-C.5 report the total energy cost trajectories and regulatory penalty shares for each fuel pathway under the three price scenarios (S-low, S-mid, S-high); Table C.1 summarises the arc elasticity statistics by fuel, and Table C.2 provides the reference market prices adopted as of May 2026. For the methane slip sensitivity, Figure C.6 reports the total energy costs, regulatory penalty share, compliance map, and energy cost variations across the three methane slip scenarios (S_1–S_3); Table C.3 summarises the technical parameters and key economic indicators for each scenario, and Table C.4 reports the arc elasticity at the reference years. All figures follow the graphical conventions established in the main text; shaded bands represent the scenario range (S-low to S-high) unless otherwise indicated.

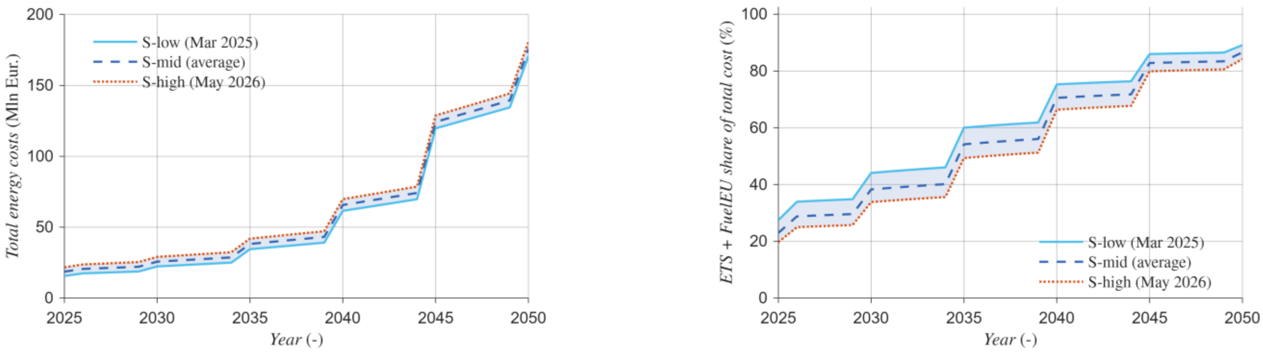

a) Total energy costs: HSFO **b)** Penalty share: HSFO

Fig. C1 Fuels prices sensitivity analysis: HSFO

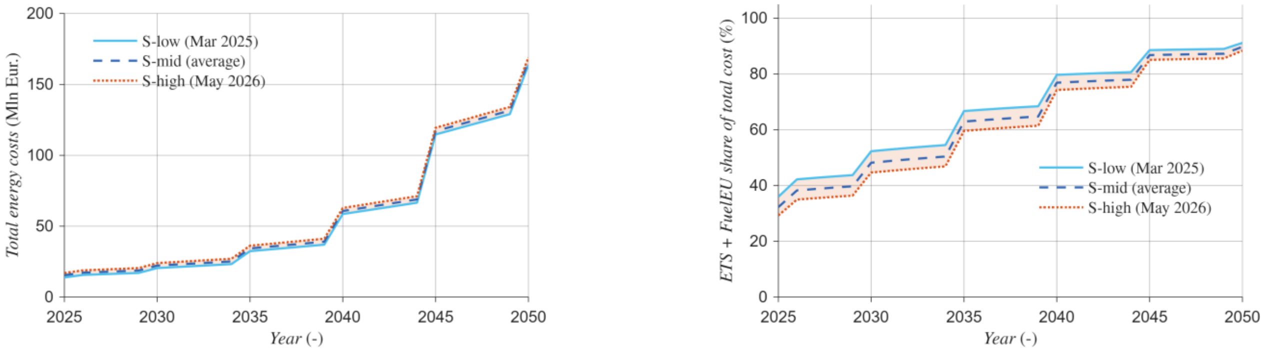

a) Total energy costs: LNG **b)** Penalty share: LNG

Fig. C2 Fuels prices sensitivity analysis: LNG

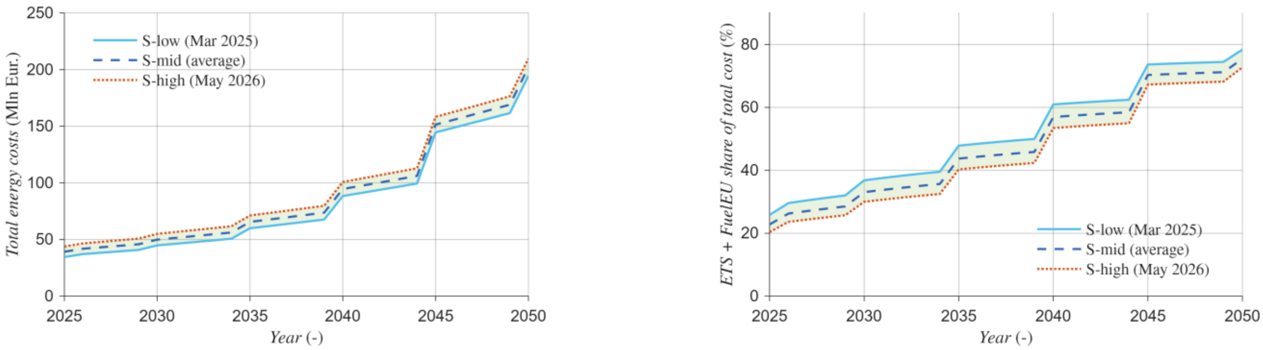

a) Total energy costs: MeOH **b)** Penalty share: MeOH

Fig. C3 Fuels prices sensitivity analysis: LNG

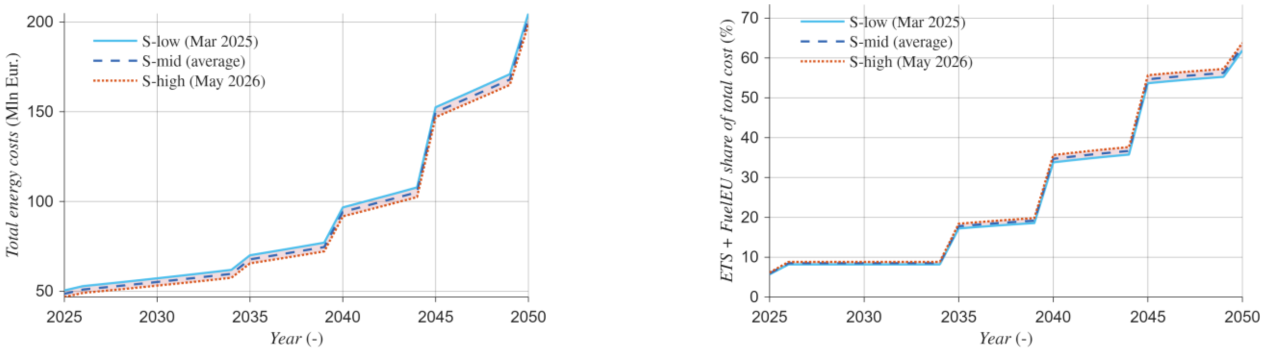

a) Total energy costs: bio-MeOH **b)** Penalty share: bio-MeOH

Fig. C4 Fuels prices sensitivity analysis: bio-MeOH

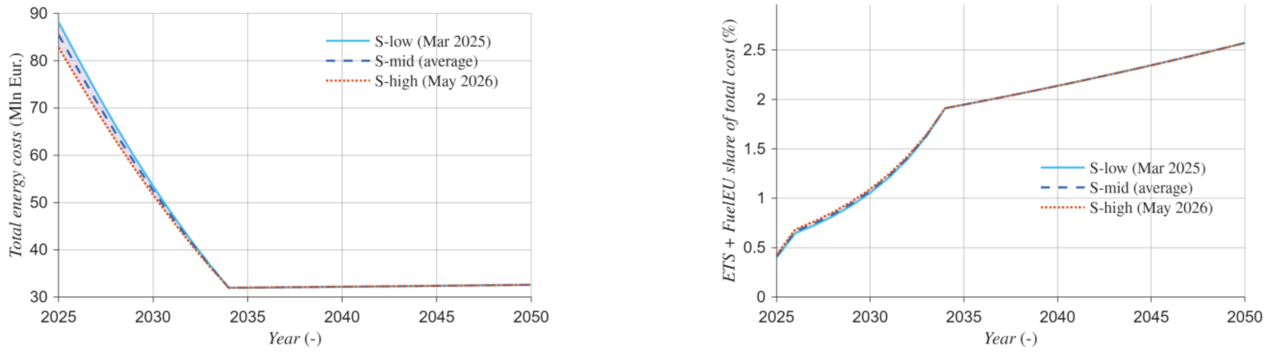

a) Total energy costs: e-MeOH

b) Penalty share: e-MeOH

Fig. C5 Fuels prices sensitivity analysis: e-MeOH

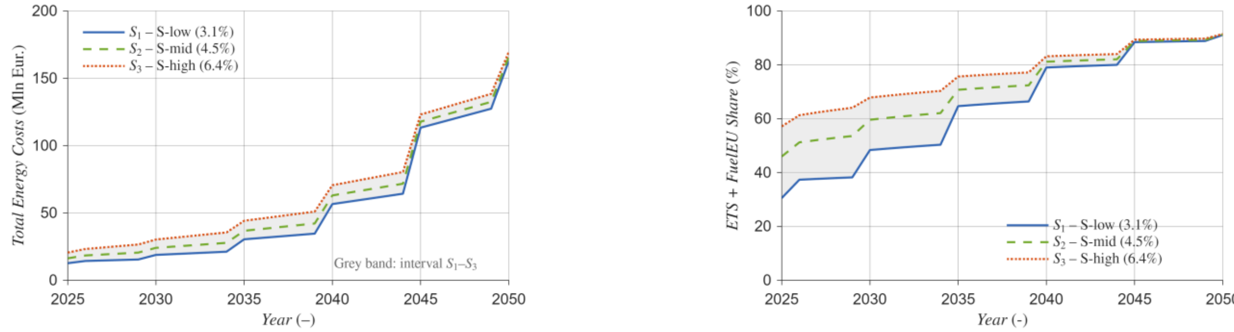

a) Total energy costs

b) Penalty share

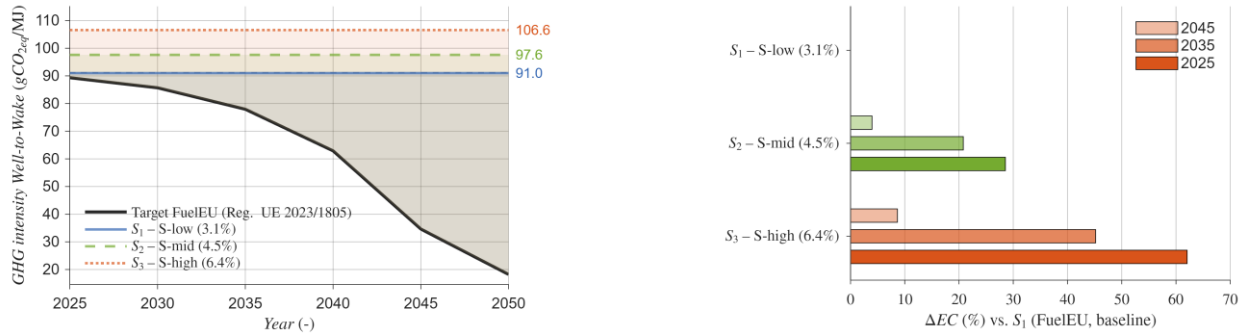

a) Compliance map

b) Energy cost variations

Fig. C6 Methane slip sensitivity analysis

Table C1 Arc elasticity: statistics by fuel

Fuel	Mean E_{fuel}	Min E_{fuel}	Max E_{fuel}
HSFO	0.436	0.134	0.773
LNG	0.360	0.103	0.679
MeOH	0.521	0.246	0.773
Bio-MeOH	0.731	0.371	0.937
e-MeOH	0.979	0.946	0.993

Table C2 Price of the fuels tested as of May 2026

Fuel	HSFO	MGO	LNG	MeOH	Bio-MeOH	e-MeOH
Price [€/t]	635	1,392	652	850	1,110	2,100 (2025) 1,325 (2034)

Table C3 Scenario Summary: Technical Parameters and Key Indicators

	S_1	S_2	S_3
C_{slip} (%)	3.1	4.5	6.4
GHG WtW (gCO_{2eq}/MJ)	91.0	97.6	106.6
Non-compliant from	2025	2025	2025
EC 2025 (Mln €)	12.76	16.35	20.65
EC 2050 (Mln €)	162.86	166.00	169.60

Table C4 Methane slip arc elasticity

Year	E_{slip}
2025	0.68
2030	0.55
2035	0.40
2040	0.25
2045	0.15
2050	0.06